DESIGN AND MANUFACTURE OF A TAPER THERMOSYPHON DRILL FOR DRY DRILLING OPERATIONS.

By

NKOSANA NCABA

218053206

A dissertation submitted to the faculty of Engineering and the Built Environment in fulfilment of the requirements for the degree of

MASTER OF PHILOSOPHY

In

MECHANICAL ENGINEERING

At the

SUPERVISOR: PROF T.C. JEN

CO-SUPERVISOR: DR K. UKOBA

05 NOVEMBER 2020

PLAGIARISM DECLARATION

I, Nkosana Ncaba, hereby declare that this dissertation is wholly my own work and has not been submitted anywhere else for academic credit either by myself or another person. I understand what plagiarism implies and declare that this dissertation is my own ideas, words, phrases, arguments, graphics, figures, results and organization except where reference is explicitly made to another's work.

I understand further that any technical academic behavior, which includes plagiarism, is seen in a serious light by the University of Johannesburg and is punishable by disciplinary action.

Date……. Signed……

ABSTRACT

Previous studies have indicated that the use of metal working fluids is harmful and poses health risks, also indicating that they are increasingly expensive. There is a drive to look for more environmentally friendly methods of machining, one such being the option of removing the need to use metal working fluids to cool off drill bits. There are studies which have highlighted the option of dry drilling without use of metal working fluids. Dry drilling has been researched and methods such as the minimal use of cutting fluid have proved to reduce the temperature of the drill bit during drilling to a certain extent when compared to the full use of metal working fluid. Dry drilling introduces options which include the use of a thermosiphon for reducing temperature of the drill bit tip, during drilling operations. The use of thermosiphons has been proved to be the most effective in cooling drill bits for dry drilling. This study focused on the design, manufacturing and testing of a reverse tapered thermosiphon, which is efficient for evaporation and condensation within a drill bit for dry drilling operations. The methodology consisted of a virtual design and a stress analysis conducted on the reverse tapered thermosyphon through the use of SolidWorks software. The stress analysis conducted on the drill bit demonstrated optimal positions of the largest diameter of the taper thermosyphon and distance from the cutting edge. The Von Mises Stress was 39 MPa and Maximum Temperature was 370℃ for an optimal cutting distance of 12 mm from the drill bit cutting edge. The drill bit also experienced a Von Mises Stress of 17 MPa and a Maximum Temperature of 433℃ and thus resulted on a large diameter of 4.7mm. The reverse tapered thermosiphon was designed for insertion within a drill bit, considering the large and smaller diameters over the length of the drill bit. This design considered the stress analysis conducted based on the simulation results on performance of the drill bit. The drill bit was manufactured for real life testing conditions, the design informed by the simulation conducted. An Electric Discharge Machining process was utilised for the creation of a cavity through spark erosion, followed by a thermosyphon of reverse taper. The drill bit thermosyphon inserted within the drill, brings a challenge in that the drill bit web thickness is 30-40% of the drill bit diameter. Such a problem is known to be more critical when it comes to long series drill bits. This was however averted by the use of an armour piercing drill bit with a larger web thickness. Three tests were conducted for the metal working, dry drilling and thermosyphon drilling conditions, using high speed drills on a drilling machine. The metal working drilling condition displayed results of exit temperatures peaking at 77℃, which was expected due to the presence of a cooling agent. The dry drilling condition displayed results of exit temperatures peaking at 421℃, with the

drill bit edges badly affected. The thermosyphon drilling condition displayed results of exit temperatures peaking at 202℃, which was far better than the dry drilling process. This result is expected to advance the technology of drill bit and help eliminate the environmental risk, health hazard and high cost of metal working fluid.

PUBLICATIONS

Published Conference Paper

1. Ncaba, N. I. *et al.* (2020) 'Effect of Thermosyphon Limits on Design of A Taper Thermosyphon Drill for Dry Drilling Operation', *Proceedings of 2020 IEEE 11th International Conference on Mechanical and Intelligent Manufacturing Technologies, ICMIMT 2020*. IEEE, pp. 118–124. doi: 10.1109/ICMIMT49010.2020.9041213

ACKNOWLEDGEMENTS

I would like to first off thank my Lord and savior Jesus for giving me an opportunity to do this research work. I am grateful for my family especially my wife and sons who are a constant inspiration for why I do this work. My extended family from Ncaba and Mahlangu who play a key role in encouraging and believing in me. To my mentor and Supervisor Prof Jen who has guided me through this work and played an important role in ensuring that I do my best. I would also like to mention my Co-Supervisor Dr. Kingsley who has been instrumental in ensuring that I meet the requirements of the University and understand research. I would also like to extend my appreciation to Machine Cutting Services Operations (Pty) Ltd, staff and management who have been of great help in allowing me to carry out tests within their workshop. I would not have been able to complete this Masters without the contribution of fellow research colleagues within the group of Prof Jen who are an inspiration.

To the African child: do not undermine your worth and do not give up on your hope and aspirations. Everything can be achieved if you attempt it.

Table of Contents

List of Figures

List of Tables

Chapter 1: Introduction

1.1 Introduction

The world is on a drive to "go green" in search for environmentally friendly methods of conducting machining activities such as drilling, milling. The use of metal working fluids within machining industries has proved harmful and as such posed health risks towards employees [1]. Numerous reports estimate that in the year 2025, the market size globally towards metal working fluids will reach levels of around 3500 kilotons in volume [2]. Studies also show that more than 85% of the metal working fluids that are utilized around the globe are categorized within petroleum –based mineral oils [2]. There are growing concerns in how this petroleum based mineral oils negatively affect the atmosphere. Studies also estimate that due to spills, improper handling, injuries, instability and total failure applications, over 50% of all the metal working fluids used around the globe enter the atmosphere [3]. Metal working fluids however produce harmful substances, such as mists emitted where machining takes place, mists when inhaled cause illnesses to operators. The focus of this study is on the machining process of drilling and the use of metal working fluids.

Metal working fluids continue to affect employees within machine shops whilst environmental costs of handling also increase. The challenges in the use of metal working fluids have proved to be costly for employers and as such there is a need to seek environmentally friendly methods. The primary focus of this study is in the use of a thermosyphon drill bit to avert the use of metal working fluids. A study conducted by Sequeira and Jen [4] focused on a gravity based thermosiphon for dry drilling application as opposed to the use of other drilling directions, i.e. horizontal, etc. The removal of metal working fluids from the machining process, bring about the challenge of adhesion at the cutting tool for materials such as aluminium where higher temperatures are employed [5]. Build up edge tends to form due to higher temperatures for such materials. In order to address this phenomenon, the use of coating cutting tools in dry machining assists in hardening the cutting tools and further reduce friction. The material that is commonly applied in such cases is solid lubricant coating is molybdenum disulfide (MoS_2), which tends to improve the properties of the cutters [5]. The absence of metal working fluids can thus be averted with the improvement in cutting tool life due to reduction in tool adhesion and friction. Coatings on coated drill bits, such as tungsten carbide, diamond like carbon, etc, assist in the reduction of friction, also to note is the use of minimum quantity lubrication which

when used in conjunction with dry machining has advantages [6]. One of the other methods of coatings that are utilized is the Oerlikon Balzer coating where high loads and high speeds are utilized, such coatings are useful in improving tool life [7].

The results proved true to the proposal of the effective gravity assisted position, which supports the vertical direction of the drill bit. The limitation in a gravity assisted position are part of what this study seeks to improve upon. Jen *et al.*, [1] proved that the use of a thermosiphon had more advantages when compared to the use of a heat pipe within a twist drill. They also highlighted the disadvantage which is the fact that a thermosyphon must be used in a vertical position to be able to operate at its best. This was highlighted due to the limitation in the type of drill bit and the geometric limitations of the drill bit flute.

One of the studies conducted [8], demonstrated that the size of the drill bit was not large enough to contain a taper thermosyphon within the drill bit. The study also highlighted concerns on the working fluid within the thermosyphon, which includes the fact that a 0.25 ml fluid was insufficient for evaporation and condensation within the thermosyphon. The study further highlighted the fact that the cap housing the fluid for proper evaporation needs to be investigated for an efficient enclosure. It was also mentioned, that it is difficult to ensure that the heat pipe is located closer to the drill tip due to the diameter of the heat pipe being affected by maximum stress levels in the drill and this affects how much it is able to cool the drill tip[9]. This study also considered the limitations in the design and insertion of a heat pipe or thermosyphon within a drill bit, as the closer it gets to the drill bit edge, the drill bit material is compromised.

It is therefore necessary that the study focused on the extent that the thermosyphon could be brought closer to the drill tip as it affects the level of cooling. This study hence investigated the use of a taper thermosiphon for optimal results, focusing on the optimization of a thermosyphon for effective dry drilling operations. The effective use of the working fluid within the thermosyphon on an optimal drill bit geometry was simulated. The study also investigated the enclosure of the thermosiphon drill for efficient evaporation and condensation process. The study considered the restrictions of the gravity based drilling orientation in order to ascertain drilling outside of gravity based orientations.

1.2 Purpose of the Study

The purpose of this study is to design a taper thermosyphon drill that is effective for dry drilling operations, which is an alternative method eliminating the need to use metal working fluids. And also to manufacture a drill that has a reverse tapered thermosyphon installed within the drill bit for dry drilling operations. The manufactured reverse tapered thermosyphon was tested in real conditions on a drilling machine in order to gauge the performance of a thermosyphon when drilling on a block of steel. The study aims to research the difficulties in the design of a taper thermosyphon to cool the drill bit on dry drilling operation. Also, it aims to consider the enclosure of the taper thermosyphon on a drill bit, to maintain the evaporation and condensation process, using a cap on the end of the drill bit shank.

1.3 Problem Statement

Previous studies have revealed that thermosyphon are efficient in cooling the drill bit tip on dry drilling operations [1]. These studies have sought to manufacture a thermosyphon for drilling operations. It was therefore discovered that it is difficult to manufacture a taper thermosyphon within a drill bit. Some of the researchers have tried to manufacture a taper thermosyphon, [8] but these were not as successful due to the same issue of the difficult process of manufacturing a taper thermosyphon within a drill bit. A study [8], also found that the thermosyphon insertion had limitations due to drill size, and thus made it difficult to manufacture a taper thermosyphon to the required dimensions of a 1 degree on a length.

It was also mentioned [1], that the taper thermosyphon is the most effective for evaporation and condensation thereby effecting efficient cooling of the drill bit tip. This study aims to design a taper thermosyphon for dry drilling operations in the pursuit of an environmentally friendly method of drilling. The study aims to focus on a manufacturing process to ensure that a taper thermosyphon is inserted within a drill bit for efficient evaporation and condensation in dry drilling operations.

1.4 Research Questions

i. What is the optimal design for a reverse tapered thermosyphon for dry drilling operations?

ii. What is the suitable method to manufacture a reverse tapered thermosyphon for dry drilling operations?
iii. What will be the performance of a reverse tapered thermosyphon when tested in real conditions of dry drilling operations?
iv. What are the optimum dimensions of a taper thermosyphon within a drill bit for effective cooling?

1.5 Objective

The objective of this study is to design a reverse tapered thermosyphon that has the required dimensions to carry out evaporation and condensation within a drill bit for cooling of the drill tip on dry drilling operations. It is to find a manufacturing process that is suitable to insert the reverse tapered thermosyphon within a drill bit in order to carry out dry drilling operations. The manufactured drill bit was tested in order to evaluate the performance of the reverse tapered thermosyphon in real life drilling operation.

1.6 Specific Objectives

i. To determine the dimensions of a taper thermosyphon for effective cooling of drill bit tip.
ii. To develop a concept through Solid Works and Finite Element Analysis (FEA) for 3Dimension (3D) modelling of a drill bit thermosyphon.
iii. To determine the optimal conditions of the tapered thermosyphon for the location of the taper and distance from the drill bit tip.
iv. To manufacture a drill bit that has a reverse tapered thermosyphon as per the design of the thermosyphon drill bit.
v. To carry out testing of the manufactured drill bit with a reverse tapered thermosyphon on a radial arm drilling machine and determine the performance on drilling a series of holes on a work piece.
vi. Determine the capability of the reverse tapered thermosyphon to cool a drill bit tip on dry drilling operations.

1.7 Preview of Literature

A formal literature review was conducted, looking at the work conduct on previous research on Heat Pipes and Thermosyphons. The literature further considered the operations of dry

drilling and the effect of metal working fluids in such operations. The study determined the effect of Thermosyphons in wicking away heat from drill bit tips. The study further drew gaps with regards to limitations in past designs of thermosyphons and thus forge a way forward pertaining to new design requirements. A comprehensive discussion of the literature reviewed is presented in chapter two of this thesis.

1.8 Experimental Design

The performance of a thermosyphon has been previously tested on parallel thermosyphons and more so on heat pipes. A study[1], conducted led to a manufacturing of a thermosyphon with a parallel bore within a drill bit and achieved a reduction in temperature of drill bit tip. The experiment concluded on the advantages of dry drilling, such as the extension of tool life. This study extended on this, through the design of a reverse tapered thermosyphon as opposed to the parallel thermosyphon. Drilling was be conducted on a conventional radial drilling machine in order to simulate a real-life situation.

The temperature was evaluated during this process of drilling on block of steel for testing purpose. The reduction in temperature was assessed to prove the results achieved on previous studies. Heat pipes have been proven to be much more complicated to install within drill bits. Figure 1 depicts the process flow of the testing method conducted in this study.

Figure 1: Process Flow of Testing Process

Chapter 2: Literature Review

2.1 Introduction

This chapter detailed the history of metal working fluids and the impacts that they have had on machining operations in particular drilling. The literature looked further at options available to avert the impacts of metal working fluids, thereby introduce the use of heat pipes and thermosyphons. This therefore gave a guide pertaining to the limitations of current heat pipes and thermosyphons.

2.2 Machining

There are various processes of cutting metal, i.e. sawing, shearing and blanking; slicing through the use cutting saws and grinders; laser cutting, water jets, sonic, etc; milling, drilling, planning, broaching, turning, and grinding, which all are varying machining methods [10]. Metal cutting has been studied broadly since its theories were brought about by Iain Finnie and an extension by Frederick Winslow Taylor who brought the theory of tool life prediction [10].Taylor had a proposal for the relationship on cutting speed and tool life [11] and the equation is as follows;

$$V \times T^n = C \tag{2.1}$$

Where:

V = Cutting Speed

T = Tool Life

C and n = Constants

Tool life extension is sought after on machining activities. Gorczyca [11] carried out an experiment demonstrating tool life against cutting tool speed and found that at a reduction in speed till 91.44 m/min, the tool life would have decreased to 50.50 min as shown in Table 1. He also plotted a graph of the cutting speed against the cutting tool life which determined the Taylor constant of n as 0.25 and C as 800 on Figure 2. On this experiment, Gorczyca used a carbide tool for machining on an alloy steel, this reflection on tool life will be explored later for a drilling activity, which will be critical in determining cutting tool life.

Table 1: Relationship between Cutting Speed and Tool Life

CUTTING SPEED		TOOL LIFE
Ft/min	**m/min**	**min**
600	182.9	3.16
500	152.4	6.55
400	121.9	16.00
300	91.44	50.50

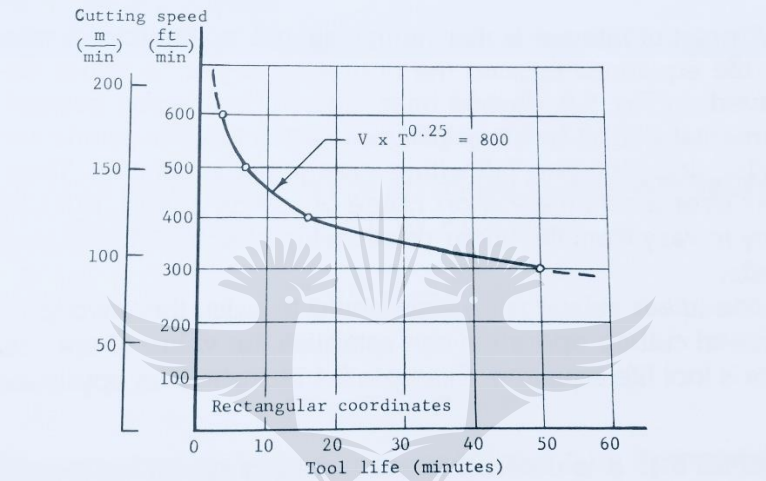

Figure 2: Cutting Speed vs Tool Life Experimental Data [11]

Metal working fluids are used to reduce the high temperatures experienced during friction when cutting or machining. Due to machining, the cutting tool tends to experience wear due to high temperatures when machining takes place. The energy that is experienced when friction occurs in machining is converted to heat and this is on the rake face of the cutting tool. Metal working fluids are used to counteract the frictional force experienced and the fluid acts as lubrication [12]. They fulfil the function of minimizing heat in the cutting environment, enhance the life of the tool, reducing work piece thermal deformation, reduction of cutting forces, preventing the tool's built up edges and improving the product's surface finish [2]. The focus of this study is on the drilling activity within machining, drilling and tapping are generally conducted at low cutting speeds. This is a functional area where metal working fluid functions as lubricants and this will be explained further on Metal Working Fluids.

Drilling holes bring a challenge of cutting chips causing friction through the drill bit flutes, when seeking to exit. They tend to clog the drill bit flutes and this causes an increase in torque and axial force, which further causes heat and marring of the hole wall surface [12]. Metal working fluids are resourceful in such cases as they wash away the cutting chips, thereby avoiding clogging of the hole being drilled.

2.3Metal Working Fluids (MWFs)

2.3.1 Background

Metal working fluids have to fulfill requirements for the removal of heat from a cutting tool, lubrication of the cutting tool and the removal of swarf from the cutting tool and material being machined [13]. The composition of these fluids must fulfil the requirements stated, and the advancements have had to accommodate the various materials in machining. Increases in performance of machining process such as speeds and feeds, on tough alloy steels, have overworked metal working fluids[14]. There are disadvantages when it comes to metal working fluids, but they also have advantages such as increased tool life, quality within work pieces to be machined, cutting tool life is also increased and better management of metal chips [12]. This then further brought about improvements in the properties of metal working fluids, which brought about characterizations of metal working fluids.

2.3.2 Metal Working Fluids(MWFs)Categories

Metal working fluids are categorized as shown in Figure 3 based on their compositions.

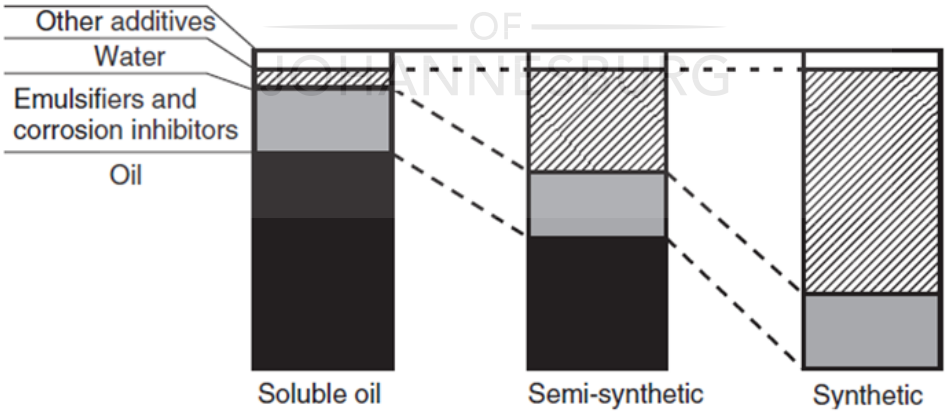

Figure 3: Relative proportion of water, oil and additives in water soluble MWFs [15]

The four categories are explained as follows;

- Straight Oils: These types of are characterized by having petroleum or vegetable oil base and can have special additives or not. They are applied in areas where lubrication is a requirement. They are mostly undiluted as they are pure oils, and this gives them the best properties for lubrication, corrosion protection and have a good resistance to

biodegrading [16]. These are rather weak in cooling abilities when compared to the water-based metal working fluids.

- Soluble Oils: These types are characterized by being water-soluble and therefore consist of a ratio between water and mineral oil. This also consists of certain additives and emulsifying agents. They are also good in cooling properties but less efficient when compared to the semi-synthetic and synthetic oils. The strength of the soluble oils is in their lubricating ability [16]. They have maintenance issues such as losses due to evaporation and growth in bacteria [12].
- Semi-synthetic Oils: These are also characterised by having the qualities of soluble oils and synthetic fluids. This means that they possess the lubricating properties, their performance is also good and they have resistance to biodegrading [16]. The other aspect of the synthetic oils is that they have a very good cooling capacity.
- Synthetic Oils: The synthetic oils do not have any mineral oils within their properties. They possess a mixture of a high content of water and organic substances together with additives [16]. They are also different in that they are cleaner and have good lubricating ability. The other qualities are that they are corrosive resistant and can conduct heat well.

These groups of metal working fluids demonstrate improvements and cooling abilities of mostly synthetic oils which are often used within drilling applications.

2.3.3Environmental Impact

The USA National Institute for Occupational Safety and Health (NIOSH) determined that metal working fluids may enter persons in ways such as when inhaling mists, aerosol or vapors which are developed when machining takes place, through direct skin contact, in particular on hands and forearms, through cuttings and abrasions, or through the mouth when workers eat or drink in the workplace without hands washed [17]. The USA Environmental Protection Agency (EPA) has discovered that the use of metal working fluids falls within the high exposure category [10]. Metal working fluids also pose disposal issues, due to the environmental regulations that companies must adhered to, to ensure disposing without causing harm to the environment. The used metal working fluid contains pieces of shavings or swarf, and other debris, which makes it challenging to dispose. The contaminated used metal working fluid tends to create an environment where bacteria breeds and this can be hazardous to machinists [18]. Part of the contamination is also a mixture of several chemicals and these require

treatment and disposal. This is done by several physical and chemical methods which are compounded by biological methods [16].

It is reported that the machining industry recorded large usages of metal working fluids, with the market at 1100 million USD, and this is estimated to increase to 1500 million USD by 2020 [19]. The high usages of metal working fluids display the levels of exposures that employees within company's experience on a regular basis. Studies further reveal that the metal working fluids tend to get contaminated as they are utilized for machining purposes, they are then disposed to the environment. The usage of metal working fluids account for 16.9% of the costs in machining, studies have recorded [19]. Regulation of exposure limits and protection to workers become key in ensuring compliance for safe work practice. There has been a drive to reduce the impact of such harmful substances to the environment. The Occupational Safety and Health Administration (OSHA) has done just that, by setting the allowable exposure limit of 5 mg/m^3 for mineral oil mist in the air, over an 8 hour average period [20]. Companies are therefore burdened when it comes to handling of these metal working fluids which continues to be expensive.

2.3.4Harmful Effects

Employees come to contact with metal working fluids during various machining processes when they are used for cooling/lubricating purposes. Employees tend to inhale aerosols or also during skin contact, such as when they touch machinery, or areas which are contaminated within workshops. Aerosols are essentially mists and they have liquid particles which are in size less than 20µm [21]. Whenever machining is being carried out and metal working fluids are applied, vapor is formulated when contact between the metal and the liquid is made, due to the heat generated from the machining [21] and this vapor forms mist when it is condensed. The non-aqueous elements in cutting fluids such as biocidal additives are then converted into a fine aerosol that can penetrate the air at the work place. Such risks impact worker's health because they can inhale the airborne vapor and as such contribute to the vapor stored within their respiratory systems regions as vapor forms mist when it is condensed. The mixture of the chemicals such as Sulphur dioxide and carbon monoxide and the air affects the health of the employees. There has been several other epidemiological reports which have indicated that the exposure to cutting fluid mist also increases the risk of airway irritation along with diseases such as chronic bronchitis, asthma or laryngeal cancer[21].

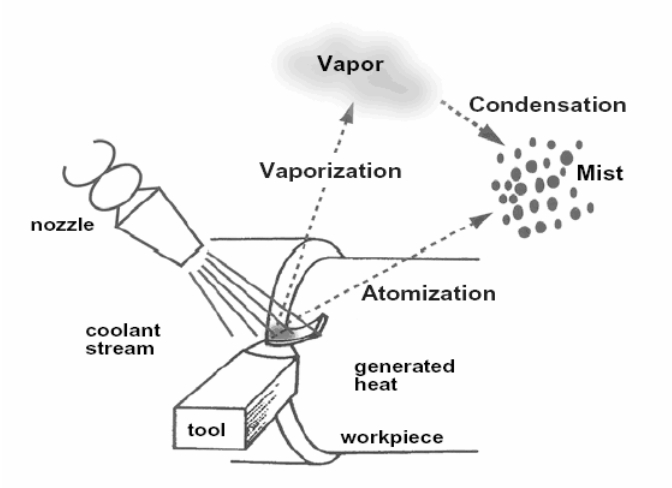

Figure 4: Cutting fluid mist generation mechanisms [12]

Figure 4 shows the process where mist is generated on a cutting tool machining onto a work piece. This is through the application of metal working fluid through a nozzle towards the cutting area where friction takes place. Evaporation and condensation takes place from heat generated by friction on the cutting tool and work piece following a jet of metal working fluid sprayed onto a rotating work piece [12].

Activities such as machining on a center lathe or milling machine, lead to metal working fluids to splash on machines, therefore aerosol tends to be deposited on the skins of machinists. Aerosol or mist emitted during processes such as drilling, machining, milling, etc. causes threats to the environment and potential hazards to workers [20]. Health hazards due to evaporation, atomization, drag out processes or whenever metal working fluids are splashed out, account for 20 – 30% [21]. Illness such as throat, pancreas, and rectum cancers can be caused by inhalations of mist. Kumar *et al*. [21] conclude that more research is still needed to optimize the use of metal working fluids with required machining performance. Breathing gases resulting from the thermal decomposition of polyfluoroethylene have caused respiratory harm to the machinists who conduct high speed machining in machine shops[22]. Chemicals such as hydrogen sulphide, phenols, ozone, nitrogen dioxide, etc. are thought to reduce resistance to respiratory infections by impairing antibacterial protection mechanisms in the pulmonary.

Often known to cause a disease as lipoid is the inhalation of oils, this great danger is due to the mineral oils. One of the challenges that arise in the use of metal working fluids is the

quantification of the volume of liquid aerosol that is contained by the filter in the air (determination of concentration in mass) during the sampling process [16]. The sensitivity of metal working fluid to aerosol is frequently associated with chronic bronchitis inflammation, hypersensitive pneumonitis and the worsening of known respiratory conditions such as asthma. This sensitivity is experienced in most machining applications such as drilling, milling, turning, etc. within machine shops. Employees continue to experience respiratory conditions and mostly are not reported as they continue to focus on required production.

2.4Cooling methods

2.4.1High pressure coolant technique

The concept of the high pressure coolant has the potential to be a good solution where high speed machining is used for achieving intimate chip-tool interaction [1]. This type of high speed machining is for speeds which do not exceed values of DN 500000. Excessive speeds would require MQL process to be utilized. The method is also useful for machining efficiency, improving cutting tool life, and the control of metal chips [20]. The temperatures at the cutting tool point is also lowered whilst improving the work piece surface area. The use of high pressure coolant technique reduces built up edge significantly during machining under normal cutting conditions. The method is efficient as there is a high pressure or compressed metal working fluid that is applied directly to the work piece and cutting tool contact area [20]. The injection of high pressure coolant technique does not only provide a reduction in cutting forces and temperature but it also reduces the consumption of metal working fluids by 50% [1].

2.4.2Air vapor and gas coolant

The method of air vapor and gas coolant is known to be the cleanest and also the most environmentally friendly cooling technique when it comes to machining operations, this has been since the cooling medium is air[2]. The chilled and compressed air contributes to this fact due to being used for cooling in this method. Studies that have been conducted on this cooling method showed that the use of chilled air as a coolant does increase tool life. Liquid Nitrogen (LN2) is a temperature that is very low and is normally kept in containers that are in isolation under high pressure [23]. Liquid Nitrogen tends to absorb the heat that is lost from the machining process and thus evaporates to nitrogen becoming part of the air [23].The machining parameters are the ones that govern the attainment of good surface finish on the work piece when using chilled air cooling technique. Studies have been conducted in the use of internal gas coolant when drilling through bovine femur and it was found that the temperatures were maintained at low levels [24]. Studies have also indicated that air cooling produces lower

surface roughness than the process of dry machining, but at the same time this method produces higher surface roughness when compared to the use of minimum quantity lubrication (MQL) or emulsion coolant [2].

2.4.3Cryogenic coolants

The method of cryogenic machining is a machining operation that is conducted at very low temperatures and these are below 120 K (-153℃) and is shown in Figure 5 [25]. This method of machining a super cold medium in mostly liquefied gases such as Nitrogen, helium, neon, oxygen and normal air, is supplied to the cutting zone for the reduction of cutting temperature, this therefore cools down the cutting tool and work piece [2, 20] . The cryogen medium removes heat at the cutting zone by absorption and thus evaporates to the atmosphere. The most used within cryogen coolants is liquid nitrogen and helium which are made from air, this therefore leads to the definition of cryogen coolants not considered to be pollutants to the atmosphere [2]. Since nitrogen tends to disappear in the atmosphere after cooling the cutting zone, the nitrogen therefore does not cause harm to workers within machining workshops.

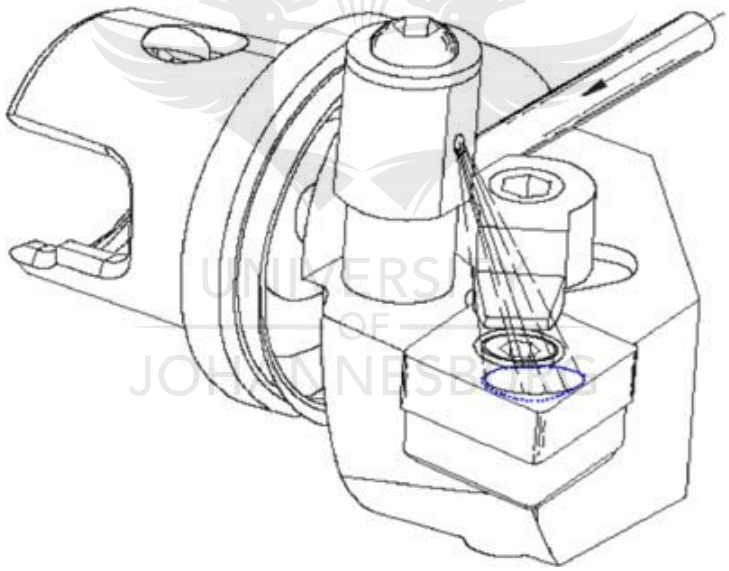

Figure 5: Cryogenic cooling method [26]

The method of cryogenic machining is usually associated with the increase in strength and hardness, cryogenic machining lowers the elongation percentage and fracture toughness of the materials and this is due to low temperatures [2]. Since cryogenic machining tends to increase the hardness of the cutting tool material, it can also reduce tool wear and thus the increase in tool life. Cryogenic cooling is known to be beneficial when it comes to the machining tough materials such as titanium and nickel-based alloys, where there is prevalence of high tool wear due to heat generated in the cutting zone [2]. The process of spraying cryogenic coolants in the cutting area when machining tough materials tends to reduce cutting temperature while also

reducing tool wear and this then grants the results of increasing tool life. This method also reduces the formation of built up edges which is formed as a result of low temperatures, and this then results in improvements in surface finish of the machined parts [2].

Ucak and Cicek [27] considered the effects of cutting conditions on cutting temperature and hole quality within the method of drilling Inconel 718 using solid carbide drills. It was found on this study that cryogenic cooling brought a significant reduction in cutting temperatures. Cryogenic drilling has better performance when it comes to hole quality and surface integrity when compared to the processes of wet and dry drilling. It was also found that the process of cryogenic conditions increases the thrust force and also brings a significant reduction in tool life due to excessive metal chips. Ahmed and Kumar[28] conducted a study in the method of cryogenic drilling of Ti-6Al-4V alloy under liquid nitrogen cooling. It was thus found that cryogenic liquid nitrogen coolant has the ability to lower the cutting zone temperature which helps in the wicking away of heat from the cutting zone. This process also considered the lower thrust forces and surface roughness due to less friction and better chip breaking in cryogenic liquid nitrogen condition. This thus brought about better chipping results with an improvement in the hole quality and tool life.

2.4.4Minimum quantity lubrication (MQL) and Minimum quantity coolant (MQC)

Since dry machining has not produced good results in machining due to heat generated between the cutting tool and work piece, therefore it is recommended to use a small amount of coolants in the cutting zone to reduce the heat generated[29]. This method of supplying the small amount of coolants is called minimum quantity lubrication (MQL) or near dry machining (NDM) or minimum quantity coolant (MQC). There are two types of MQL delivery to the cutting zone namely: external delivery and internal delivery. In the external delivery lubricants is supplied by the nozzle as shown in Figure 6. The external method of delivery through the mist is thus demonstrated which further assists in the evacuation of metal chips. In the internal delivery the drill bit normally has holes from the cutting edge to the tip of the drill bit shank, this is where lubricants are directed within the drill bit in order to reach the cutting zone. The usage of cutting oil in MQL is restricted to 10 to 100 ml per hour[29]. There are different types of lubricating agents that are used in the MQL systems and they are: mineral oils, vegetable oils and nano-particles.

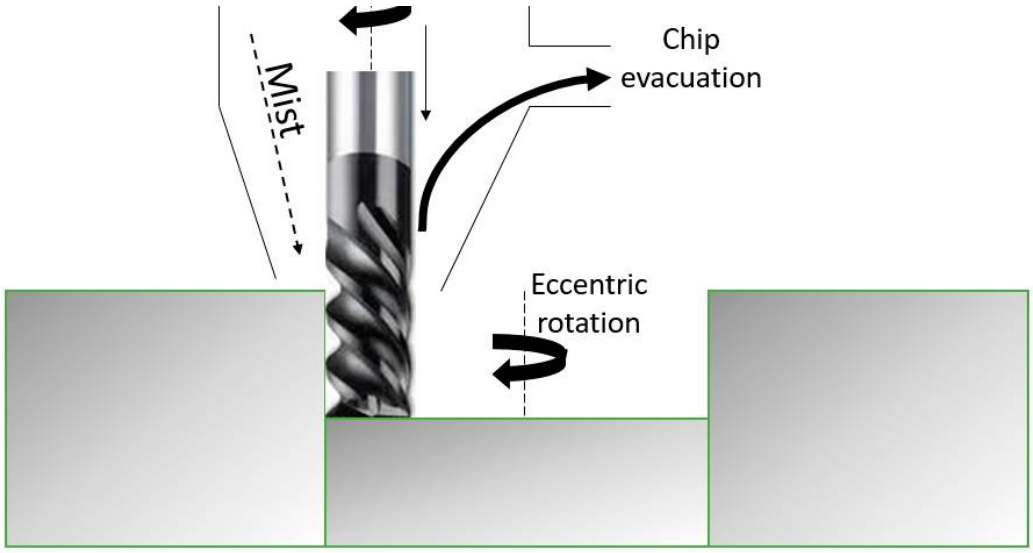

Figure 6: Minimum Quantity Lubrication method [30]

Bhowmick and Alpas [6] found that the minimum quantity water lubrication brought a reduction in drill flank wear and the degradation of coating, this is when using an HSS drill with a diamond like carbon coating in drilling of cast magnesium alloy. It was also found that the use of MQL had a requirement of less torque when compared to wet and dry drilling. The built up edge formation and adhesion of magnesium alloy to the drill tip was also reduced due to the reduced temperature in the cutting zone because of MQL. Tasdelen *et al.*[31] conducted an experiment on drilling using two cooling methods and these are: wet drilling and MQL drilling with a flow rate of 15 ml per hour. It was found that MQL had improvements in results on the surface finish when compared to wet drilling after examining the surface finish of the holes and this is when drilling 272 and 315 holes. It was also found that uninterrupted supply of MQL also produces better tool life when compared to interrupted supply.

Rahim and Sasahara[32] conducted an experiment on MQL during the drilling of Inconel 718 using two types of lubricants and these are palm oil and synthetic ester. The results were compared and it was found that palm oil showed better surface finish when compared to synthetic ester. Bhowmick *et al.*[33] conducted an experiment on the drilling of cast magnesium alloy. It was found that MQL brought an improvement in tool life and surface finish when compared to dry drilling and almost similar results to that obtained in wet drilling. This has thus brought a view on the extent of use of MQL in drilling activities, MQL has advantages since the use in coolant is not as excessive as on high pressure and other methods. Workers are however still exposed to the harmful effects of the use of coolants when using MQL, due to the exposure of the mist.

Dry machining to be discussed in the following section explains the tribological characteristics at the cutting tool and work piece interface. These further detail the differences in the machining through the use of the thermosyphon without the use of metal working fluid.

2.4.5 Solid Lubricants (MQL)

Solid lubricants are known to function in the same manner as the lubricants of liquid. They have the quality of reduction of friction and wear between materials. They are also required in areas where there is high temperatures and contact between surfaces or where there is presence of vacuum. Solid lubricants however perform better than liquid lubricants due to the properties of the solid lubricants [34]. They are classified into the two types of important groups and these are organic and inorganic. There are many applications and areas where solid lubricants are the preferred option over the liquid and semi solid lubricants. The solid lubricants are mostly preferred in industries of aerospace, air craft, outer space, marine industry, etc [34].

2.5 Dry Machining

Dry machining is a machining process in which the machining of a work piece is conducted without the use of cutting fluids applied on the work piece. This process is conducted in order to avert the health risks and environmental effects posed to employees when using cutting fluids in machining operations. Dry machining eliminates the use of metal working fluid outright thereby reducing the costs of machining and associated hazards. The use of dry machining at times present a situation where the frictional force and the cutting temperature tends to be more than that of liquid machining [21]. At times these could avail challenges to the machining process but these have been taken into consideration. The use of the thermosiphon that is reverse tapered has the advantage of the use of coolant within the thermosyphon. This is an indirect application of metal working fluid within the thermosyphon but the operator is not affected as the fluid is contained within the thermosyphon. The advantages being the fact that the fluid will continuously cool the drill bit.

2.5.1 Dry Drilling

Environmentally friendly methods of drilling are being sought, the use of metal working fluids have however motivated the need to seek alternatives [33]. Dry drilling is associated with high temperatures at the work piece and drill bit interface, this has some detrimental effects on the tool life, drilled hole accuracies, and the work piece surface finish integrity. Several studies

have however been done by researches on the study of dry drilling focusing on tool life, drilled hole accuracies and surface finish integrity.

Li and Shih [35]studied the cutting tool temperature when drilling titanium, it was found that there is a high concentration of temperature at the cutting edge of the drill tip. The drill bit temperature continues to rise with the increase in drill depth. This study also showed that the cutting edge had a lower heat partition factor and also had higher heat generation rate per length of drill than the chisel edge. The peripheral speed also increased from 24.4 m/min to 73.2 m/min after 12.7 mm depth, and as a result the peak temperature of the drill increased from 480℃ to 1060℃ [35]. The peripheral cutting speed then resulted in a further increase, and as such the location of peak temperature moved outside towards the drill margin.

2.5.2 Heat Pipes and Thermosyphon Drill

This section introduces the application of heat pipe and thermosyphon on drill operations and the associated theory and its physics of the heat pipe. The limits of the heat transfer and heat pipe performance are also discussed.

2.5.2.1 Types of Heat Pipes

There different types of heat pipes and they are; two phase closed thermosyphon, capillary driven, annular, rotating, gas loaded, loop, capillary pumped loop, pulsating, monogroove, macro and miniature, inverted meniscus and non-conventional [36]. The conception of the idea of heat pipe was by Gaugler [37]. He conceived a devise that was light in weight and was basic for that time as there was no requirement for sophisticated systems and as such little attention was paid to that device [38]. The prominence of heat pipes as reliable devices was due to results and the design tools that were discovered on heat pipes published [39]. These results then led to a worldwide increase in research work relating to heat pipes.

2.5.2.2 Heat Pipe Operation

Heat pipes and heat exchangers contribute in the reduction of the use in energy, as the world continues to use large amounts of energy in heat. Heat pipes have a high thermal conductivity, and this is coupled to a heat flux that is high, and also an apparatus that is passive in heat transfer, they therefore need no temperature gradient for efficiency in heat transfer [40]. They are normally closed pipes, as they are devices that transfer heat, they have two phases inside the heat pipe, the one side is known as the evaporator with liquid in the section, which absorbs the heat whilst the other is the condenser which normally rejects the heat due to condensation. Heat pipes are used for various purposes and one of the purposes is for electronics cooling, applications in space, heat transfer for the stability of permafrost within pipelines. Figure 7

demonstrates the flow of working fluid within the heat pipe from the evaporator section to the condenser section [41]. The heat pipe contains a working fluid, which can change in phases, being either liquid or vapor. The working fluid thus is available in various types and these are; water, nitrogen, acetone, ammonia, etc. depending on the type of application.

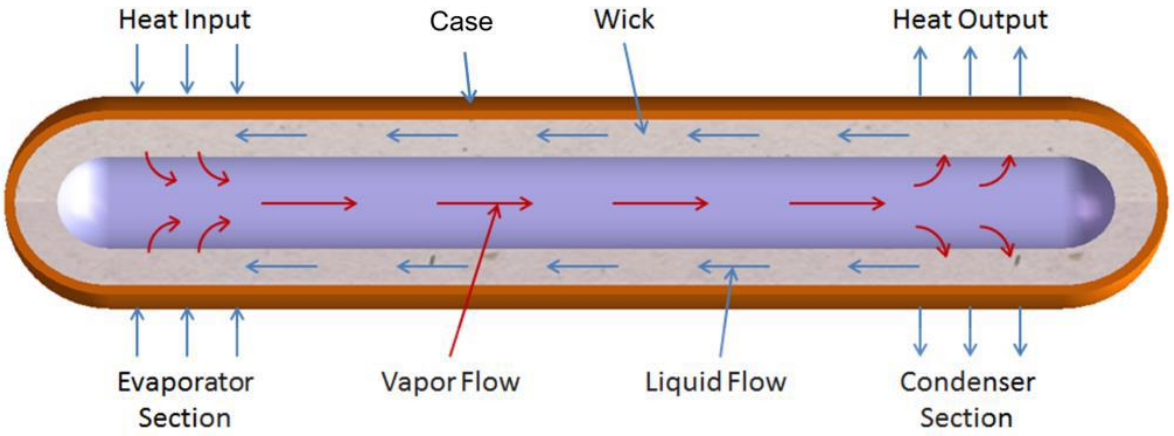

Figure 7: Horizontal heat pipe with evaporator and condenser sections displaying absorption and heat rejection in condenser [41]

The heat pipe that is conventional in cylindrical shape is displayed in Figure 7, this type, has an external case and also contains a wick structure, which is within the internal diameter of the case. The flow is thus demonstrated on vapor and liquid with heat shown in the evaporator section as input and the output of heat shown at the condenser section. This is a typical operation of a heat pipe, the distinction also being the fact that it has a wick while a thermosyphon would not have a wick. Heat Pipes also have the advantage in the ability to convey huge amounts of heat through a pipe cross section area for a significant distance, without the need to put in supplementary power. Heat Pipes are one of the most capable systems out of the many distinguishable systems that convey heat [42]. The operation of the heat pipe is natural in that the force that is used to maintain the flow of the working fluid originates from the heat transfer flow.

The functionality of a heat pipe is dependent on the heat being applied on the evaporator section, this leads to vaporization of the working fluid [43]. The vapor moves to the low condenser temperature through the adiabatic section of the heat pipe where condensation of the working fluid takes place. The latent heat of the vapor is released and as a result the vapor is converted to liquid [44]. The condensed liquid travels back to the evaporator section of the heat pipe by capillary action [38]. Whenever there is a heat sink placed at a certain part of the heat pipe, there is condensation that occurs preferably at the position of heat loss, this thus leads to

a pattern of vapor flow that is formed. The process is such that the heat pipe has the capacity to continue in transporting the latent heat of vaporization and this is from the area of the evaporator to that of the condenser. Therefore, this will proceed for a continuous duration as long as the capillary pressure is adequate for transporting the condensate back to the evaporator field [36].

The diagram in Figure 8 displays a generic heat pipe cycle, and contains the flow in sections (a) heat transfer and second section (b) diagram of the temperature versus the entropy. The position 1 displays the working fluid when approaching the evaporator section, with the condition being sub-cooled. The liquid enters the evaporator and when it is saturated it is converted to saturated vapor, thereby entering the position 2. There is more heat that is exerted and therefore the conversion is to superheated vapor. This vapor is then transported to the condenser section where heat is released, this vapor then condenses and becomes liquid now located at position 4, then the liquid moves to the evaporator section. The process from here on is driven for recirculation and as a result heat transfer takes place continuously. The heat pipe experiences a drop in temperature due to the heat that is being transferred at the wick and at the wall of the pipe material. The heat pipe as a result experiences capillarity due to the fluid flow within the wick.

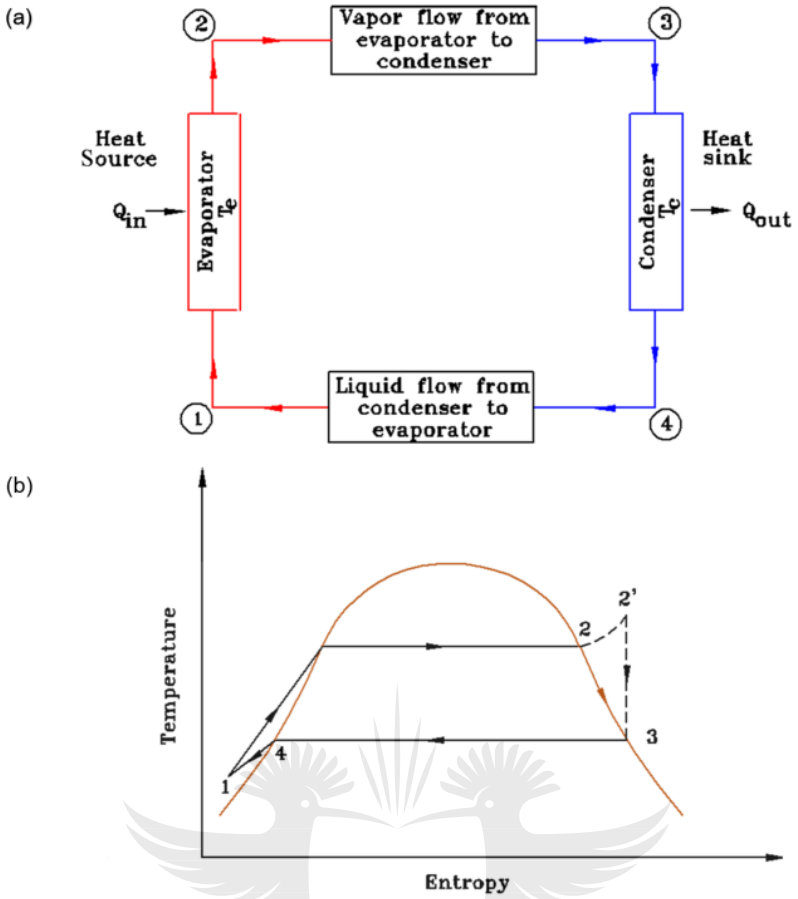

Figure 8: Graph of the temperature versus the entropy displaying the cycle of thermodynamics on a heat pipe [42]

The wick within a heat pipe has the functionality of transporting the working fluid within the condenser area to the evaporator area. A typical wick may comprise of the layers of metal screen or other metallic porous structure [45]. Typically, a successful form of wicking material seeks to optimize the fluid's flow, has constant porosity, has very tiny pores and this is in order for the wick to produce a huge capillary pressure, to avoid the degradation of the temperature and therefore does not respond or decay chemically with the liquid. A heat pipes efficiency depends on the capillary head found inside the wick, which is necessary to counteract the pressure changes involved with the movement of liquid and vapor and the gravity head [45].

2.5.3 Thermosyphon

Thermosyphons as mentioned within the Heat pipe section have a distinct difference of not containing a wick structure when compared to their heat pipe counter parts and this then brings other characteristic challenges. They are also known as two phase closed thermosyphons due to being gravity assisted and wickless with a location of the condenser above the evaporator

[36]. They therefore depend on gravity for operations, liquid is primarily driven through gravity from the evaporator section and this limits the positioning of the condenser section above the evaporator section. This allows for liquids that are of a higher quantity than when compared to the liquid contained within heat pipes. The heat transfer is known to be much higher when operations are within a vertical, gravity assisted thermosyphon, and this would as a result lead to better heat transfer than on a horizontal heat pipe. The purpose of gravity is to assist the evaporation and condensation process, since the condensate would be assisted to return to the evaporator section. Figure 9 demonstrates the pool of liquid contained within the thermosyphon at the evaporator section on a vertical orientation [42]

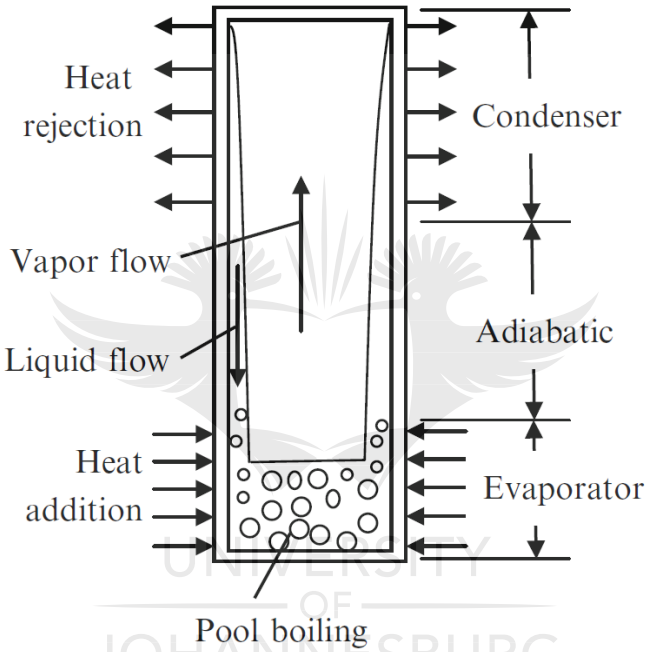

Figure 9: Vertical orientated thermosyphon with a pool of liquid within the evaporator section [42]

Gravity assists the vapor to move within the adiabatic section of the thermosyphon through the release of latent heat within the condenser section, the vapor condenses to liquid and moves to the evaporator section using the walls of the thermosyphon as liquid. The two phases that occur within the thermosyphon, lead to the thermal conductivity changing over the length of the thermosyphon, they therefore do not have a specific thermal conductivity. When it comes to thermosyphon's, gravity returns the condensate to the section of the evaporator. Although the latent heat of the evaporation is immense, a large amount of heat may be transferred from one end from another with a slight change of temperature.

The key drawback of the thermosiphon is that the evaporator area must be positioned at the lowest point in the device in order for the condensate to transported to the evaporator section through gravitational force [45]. An experimental study was conducted where the performance of the thermosyphon was evaluated for a feasibility to cool the drill bit tip [46]. It was discovered that the temperature reduction was high when a solid drill was compared to a thermosyphon drill, the reduction was in the region of 60% for an experiment conducted on a vertical position [46]. Heat pipes and thermosyphons both have the capacity to cool down drill bit tips. It was however discovered that using the thermosyphon has some advantageous when compared to the use of a heat pipe [46].

2.5.4 Operating Limits

There are specific operating limits that Heat Pipes and Thermosyphons work within and these are heat transfer limitations that they adhere to. Two phased closed thermosyphon are known as wickless heat pipes and as such are types of heat pipes with the nature of being gravity assisted [36]. Figure 10 displays a graphical representation of the limits.

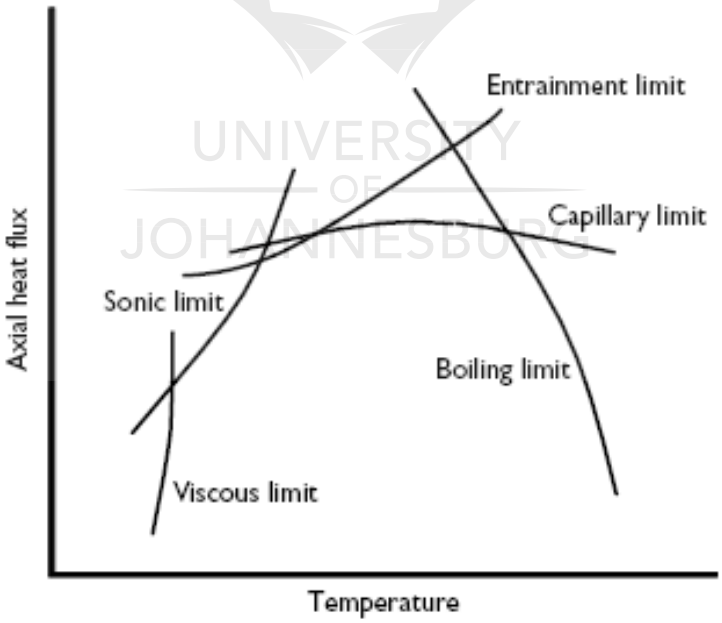

Figure 10: Limitations to heat transport in a heat pipe [47]

2.5.4.1 Vapor Pressure Limit

The vapor pressure is experienced within the heat pipe and is known as “viscous limit”. This type of limit takes place when there is a difference in the pressure between the evaporator section and the condenser section, and this is when the difference is lower than what is experienced in viscous forces. The requirement of the heat pipe that the vapor is to flow back

towards the condenser section is therefore limited due to the vapor pressure limit and this subsequently limits the rate at which heat is transferred. Therefore, the end of the evaporator section has to fulfill the condition of maximum and the end of the condenser section has to fulfil the condition of minimum. Figure 11 demonstrates the vapor pressure and how it is distributed within the heat pipe. Should the vapor pressure seen below, reach a low, within the section of the evaporator, the vapor pressure drop subsequently gets to a drastic low as well [48].

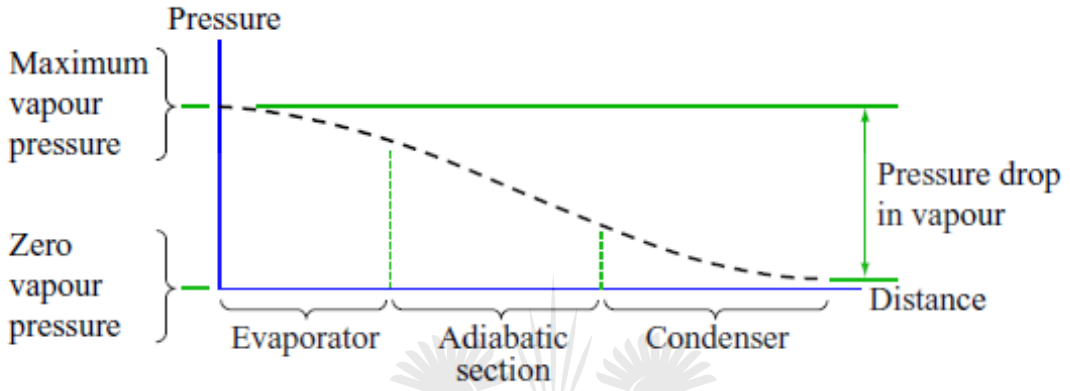

Figure 11: Limitations to heat transport in a heat pipe[48]

2.5.3.2 Boiling Limit

The heat pipe with the two sections of evaporator and condenser tends to undergo varying conditions, should the heat flux experienced radially within the section of the evaporator reach a level that is too high, it will affect the working fluid in that it will boil up and this then results in the temperature of the wall also becoming very high. The bubbles of vapor that are created within the wick of the heat pipe tend to prevent the working fluid from wetting the heat pipe wall and this results in hot spots. In the lower range of the temperature differentials the heat flux is small and this process concept of heat transfer is called free convection. During this time, when the temperature differential rises, nucleate boiling tends to dominate. On the heating surface babbles are shaped, they expand in size and tend to break off. They then come to the surface after they split free, then explode, emitting vapor [49]. The heat pipe does however have a condition where the heat flux experienced radially is rather low or moderate and in such a case the heat pipe experiences pool boiling, that is of low intensity and doesn't cause dry out. The critical heat flux of a cylindrical shaped heat pipe can be expressed as follows by Faghri [42];

$$q''_{CHF} = 0.149\rho_v h_{fg}\left(\frac{g\ni[\rho_l-\rho_v]}{\rho_v{}^2}\right)^{\frac{1}{4}} \quad (2.2)$$

Where:

q''_{CHF} = Critical heat flux (W/m^{2}K)

ρ_v = Saturated vapor density (kg/m^3)

h_{fg} = Latent heat of vaporization (kJ/kg)

g = Gravitational acceleration (m^2/s)

ρ_l = Saturated liquid density (kg/m^3)

ρ_v = Saturated vapor density (kg/m ^{3})

2.5.3.2 Entrainment Limit

The heat pipe has a shear force where the liquid interfaces with the vapor within the wick, and this is due to the opposing movements in directions of this liquid and vapor. When the relative velocity is high, there are droplets of the working fluid that tend to be torn from the surface of the wick and are drawn into the vapor that is moving towards the section of the condenser. This creates a condition where if the entrainment increases to a great extent, this will result to the evaporator dry out, and the rate of heat transfer governing this process is known as the entrainment limit. When the droplets come into contact with the condenser section of the heat pipe, they make sounds and these signal entrainments. The entrainment limit is often characterized by the temperature that is experienced by heat pipes and this is mostly low and moderate, they are also characterized by the size of the diameter which is mostly small. The entrainment limit is also characterized by temperatures that are high experienced by heat /There is a set of equations (equation 2.3 to 2.5) that are shown by Faghri [42]. They are utilized in the prediction of heat transfer based on flooding limit.

$$q_{max,flood} = \frac{T_b h_{fg} \pi {D_i}^2 \left[g\sigma\ni(\rho_l - \rho_v)^{\frac{1}{4}} \right]}{(\rho_v^{\frac{1}{4}} + \rho_l^{\frac{1}{4}})^2} \quad (2.3)$$

Where:

$$T_b = \left(\frac{\rho_l}{\rho_v}\right)^{0.14} [\tan({B_O}^2)]^2 \quad (2.4)$$

$$B_O = D_i \left[\frac{g((\rho_l - \rho_v)}{\ni}\right]^{\frac{1}{2}} \quad (2.5)$$

Where:

$q_{max,flood}$ = Maximum heat flux (W/m^{2}K)

T_b = Flooding limit parameter

h_{fg} = Latent heat of vaporization (kJ/kg)

D_i = Thermosyphon inside diameter (m)

g = Gravitation acceleration (m^2/s)

σ = Surface tension (N/m)

ρ_l = Saturated liquid density (kg/m^3)

ρ_v = Saturated vapor density (kg/m^3)

B_O = Bond number

2.5.3.2 Sonic Limit

The heat pipe with the two sections, evaporator and condenser, they represent flow channel of the vapor. The speed at which the vapor moves increases as it moves by the evaporator and this speed then reaches a maximum at the end of the section. This type of system has a limitation that has a similarity to that of a nozzle that converges and diverges, and a mass flow rate that remains constant, where exit section of the evaporator tends to correspond to the nozzle throat. There is thus an expectation that the speed of the vapor at this particular point cannot be more than that of the speed of sound. This specific condition where the flow is restricted through chocking is known as the sonic limit. The sonic limit then has a chocking effect on the amount of vapor that can flow through the heat pipe, this then limits the energy that can be transported by the vapor, this results in the limitation in the operation of the heat pipe.

2.5.3.2 Condensing Limit

There are two ways that the condenser has a method of limiting the condensate from returning to the evaporator section; the first is the rate at which the energy is removed from the system, and the second is the highest flow rate of the same condensate. Sparrow and Hartnett [50], demonstrated that there is a solution for condensation on a rotating pipe and the authors concluded on a layer similarity approach. The authors also specified restrictions in the size of the cones that apply and these are not to be too thin, stating the region from the cone that is not to be too close to its apex. The equation by Sparrow and Hartnett [50] below demonstrates the rate of the heat transfer within the heat pipe.

$$q_t = \rho_v \mathrm{u}_v A h_{fg} \tag{2.6}$$

Where:

q_t = Total heat transfer (W/m^{2}K)

ρ_v = Saturated vapor density (kg/m^3)

A = Cross sectional area for flow (m^2)

h_{fg} = Latent heat of vaporization (kJ/kg)

2.5.4 Previous work done on heat pipe and thermosyphons drilling

In a closed two-phase thermosyphon with a water-filled 20 mm OD x 17 mm ID x 2,5 m long copper thermosyphon with internal circumferential grooves, Nguyen-Chi and Groll [51] investigated the entry or flood limit. Sections of the evaporator and condenser were 1.0 m long each. The portion of the evaporator was heated with wires of electrical resistance and the condenser was cooled through a jacket of water cooling. The Fill Ratio of filled liquid length to the evaporator (FR) was between 0.38 - 0.88, 1 - 80-degree inclination angle, 20 - 80-degree evaporator wall temperature and 100 - 420-degree power input. They derived an empirical correlation to estimate the maximum performance for the inclined thermosyphon and proposed more work to be done to determine the effect of parameters such as FR, aspect ratio, pipe internal surface roughness, and working fluid type.

Gurses, *et al*. [52] conducted a study on the effect of inclination for a copper pipe with the following dimensions, 18 mm OD x 15 mm ID x 1.93 m long water-filled heat pipes for solar applications. The air-cooled condenser had an outer 400 mm diameter fins of 420 mm long. Power input up to 1200 W resulted in a temperature of the evaporator wall up to 70 °C. The study concluded that due to the entrainment limit and capillary limit, the best angles of inclination are between 45-90^{o} and depend on the power input range.

Shanthi and Ramalingam [53] conducted a study where they were experimenting with a thermosyphon assisted through two processes of gravity. The authors used a thermosyphon with dimensions, 12.5 mm ID x 300 mm long with a 200 mm long refrigerating water jacket and a 1000 W nichromeheating wire wrapped around the 75 mm long portion of the evaporator. They calculated their thermosyphon's output, concluded by plotting the efficiency as a power ratio, and resulted with values to the region of 0.9.

An experimental study [54] was conducted where the authors sought to verify the concepts of thermal management. The authors used a drill with the insertion of a heat pipe within the center, the evaporator section was located close to the drill bit tip, whilst the condenser section was

near the end. A drill, 19.05 mm OD X 247 mm long, had a 6.35 mm heat pipe inserted within the drill. It was found that on a comparison a heat pipe drill with the solid drill that there was a significant change in the temperature and this was to the range of 41% for vertical and 31% for horizontal.

Jen, *et al*. [55] conducted a numerical and an experimental study where they investigated the feasibility of the insertion of a heat pipe within a drill bit. The experimental setup prior to the manufacturing of the heat pipe drill, consisted of a steel cylinder with a 25.4 mm OD, and had a 6.35 mm ID hole within the center for the insertion of a heat pipe, and the length was 216 mm. The simulation carried out was that of a heat band of 85W on the drill bit tip. To calculate the temperatures in the cutting zone, a finite element numerical analysis was also performed. The results depicted a preliminary verification of the feasibility in cooling through the use of the heat pipe. The drills with dimensions of 19.05 mm OD and 228.6 m length were manufactured with the insertion of heat pipe for testing. The authors concluded that the numerical and experimental studies show that there is a drastic decrease in drill temperature when using the heat pipe within the drill bit.

An experimental study by Jen, *et al.* [46] sought to determine the feasibility of cooling a drill bit tip through the use of a thermosyphon. The experiment conducted was identical to the one done by Jen, *et al*. [54] following a similar procedure and use of apparatus. The drill bits that were utilized in this experiment were 19 mm in diameter and 266.7 mm long made of high speed steel. It was found that the construction of the thermosyphon was easier than that of a heat pipe and also less expensive. It was also found that the insertion of a thermosyphon within a drill bit requires a drill that is large enough. The use of a drill bit with a thermosyphon resulted in a reduction of 60% temperature of the drill bit tip when compared to the use of a solid drill bit.

Chapter 3: Design

3.1 Introduction

This chapter details the design and simulation of the thermosyphon for dry drilling.

3.2 Design Selection

The design of a thermosyphon exhibited the dimensions of a reverse tapered thermosyphon for the successful insertion within the drill bit. The dimensions of the small diameter are 2.5 mm and the dimension of the large diameter is 6.38 mm. Jen, *et al.* [46] considered a drill bit that was 19 mm in diameter for the experimental study that was conducted for a thermosyphon drill. The design of the experiment considered previous drills that were used for experiments in rotational drills. This study followed a similar approach in considering the dimensions of the drill bit and the insertion of a thermosyphon. The design also considered the thermal management abilities of a drill bit with a rotating heat pipe similar for cooling of drill bit tip as proved around 41% temperature reduction [54]. The feasibility of using drill bits for drilling through the insertion of thermosyphons is efficient and this study follows similar designed for rotating drill bit.

3.3 Design Calculations

3.3.1 Detailed calculations of the drill performance

The following calculations determine the drill bit performance required for the simulation of the drill on stress and thermal analysis. The simulation of the drill will reveal the characteristics of the drill bit for the testing and manufacturing process to be detailed on the following chapters. The selected speed is 420 RPM for the simulation tests to be conducted. The machine spindle speed [56] is calculated using the following equation:

$$N = \frac{v}{\pi D} \tag{3.1}$$

Where:

N is the rotational speed (rev/min)

v is the cutting speed in (m/mm)

D is the drill diameter in (mm)

Substituting the variables, the cutting speed of the drill bit is therefore:

$$v = \frac{\pi ND}{1000}$$
$$= \frac{\pi(420)(20)}{1000}$$
$$= 26.3894 \text{ m/min}$$

The feed [56] is calculated using the following equation:

$$f = Nf_r \tag{3.2}$$

Where:

f_r is the feed rate in (mm/min)

N is the rotational speed in (rev/min)

f is the feed in (mm/rev)

Substituting the variables, the feed is therefore:

$$f = (420)(0.0254)$$
$$= 10.668 \text{ mm/min}$$

The drilling time is calculated using the following equation [57]:

$$T_m = \frac{t + A}{f_r} \tag{3.3}$$

Where:

T_m is the machining time measured in (min)

t is the workpiece thickness in (mm)

f_r is the feed rate in (mm/min)

A is the approach allowance in (mm), and this is calculated using the following equation:

$$A = 0.5D \tan\left(90 - \frac{\theta}{2}\right) \tag{3.4}$$

Where:

D is the drill diameter in (mm)

θ is the point angle (which in this case is 118°) in degrees

Substituting the variables, the approach allowance is therefore:

$$A = 0.5 \times 20 \times \tan\left(90 - \frac{118}{2}\right)$$

$$= 6 \text{ mm}$$

The thickness of the work piece for the test is 50 mm.

Substituting the variables, the machining time is therefore:

$$T_m = \frac{t + A}{f}$$

$$= \frac{50 + 6}{10.668}$$

$$= 5.249 \text{ min}$$

The material removal rate is calculated using the following equation [57]:

$$R_{MR} = \frac{\pi D^2 f_r}{4} \quad (3.5)$$

Where:

$R_{MR}$is the material removal rate in(cm^3/min)

$f_r$is the feed rate in(mm/min)

$D$is the drill diameter in (mm)

Substitution the variables, the material removal rate is:

$$= \frac{\pi(20)^2(0.0254)}{4}$$

$$= 7.9796 \text{ cm}^3/\text{min}$$

The specific cutting force is calculated using the following equation [58]:

$$K_C = K_{C1}(f_z \times \sin(k_r))^{-mc}\left(1 - \frac{\gamma}{100}\right) \quad (3.6)$$

Where:

K_C is the specific cutting force in(N/mm^2)

K_{C1} is 1500 [56]

f_z is the feed force in the z direction and it is worked out as follows;

$$f_z = \frac{f_r}{2} \quad (3.7)$$

$$= \frac{0.0254}{2}$$

$$= 0.0127$$

Where:

k_r is the pointing angle (which is 118°) and when divided by 2 the angle is 59°.

mc is 0.25 [56]

$\gamma$is the rake angle or helix angle which is 30°.

Substituting the variables, the specific cutting force is therefore:

$$= 1500(0.0127 \times \sin(59))^{-0.25}\,(1 - \frac{30}{100})$$

$$= 3250.665\ \mathrm{N/mm^2}$$

The thrust force is calculated using the following equation [58]:

$$F_T = 0.5 \times K_C \times \frac{D}{2} \times f_r \times \sin(k_r) \tag{3.8}$$

Where:

$F_T$is the thrust force in (N).

Substituting the variables, the feed force is therefore:

$$F_T = 0.5 \times 3350.665 \times \frac{20}{2} \times 0.0254 \times \sin(59)$$

$$= 353.868\ \mathrm{N}$$

The net power required, is calculated using the following equation [58]:

$$P_C = \frac{f_r \times v \times D \times K_C}{240 \times 10^3} \tag{3.9}$$

Where:

$P_C$is the net power in (kW)

Substituting the variables, the net power is therefore:

$$P_C = \frac{0.0254 \times 26.3894 \times 20 \times 3250.665}{240 \times 10^3}$$

$$= 0.1816\ \mathrm{kW}$$

The torque is calculated using the following equation [58]:

$$M_C = \frac{P_C 30 \times 10^3}{\pi N} \tag{3.10}$$

Where:

M_C is the torque in(Nm)

Substituting the variables, the torque is:

$$M_C = \frac{(0.1816)(30 \times 10^3)}{\pi \times 420}$$
$$= 8.09 \text{ Nm}$$

3.4Finite Element Analysis on the Drill Bit

The Finite Element Method, also referred to as FEM or FEA (Analysis), is a mathematical method used in cases involving stress analysis, heat transfer, electromagnetism, or fluid flow to solve engineering problems. Differential equations are solved by applying boundary conditions to a chosen geometry using FEM, which will then explain the real-world applications of the segment in question. The feature that is most important to the use of FEM is the ability to solve differential equations over the whole area of a part, with such a part divided into smaller parts that are referred to as finite elements, these are connected through a series of nodes, with each element solved with others simultaneously [59].

3.4.1Introduction

The FEM was conducted on a 20 mm drill bit, parallel shank in order to determine the drill bit performance during drilling application, and stress and displacement was determined. A stress and thermal FEM conducted determined the baseline values that would be utilized later in this study.

3.4.2 Drill Bit Performance

The drill bit material properties of an M2 high speed steel to be used for the testing process are as shown on Table 2:

Table 2:M2 High Speed Steel Material Properties

Property (Unit)	**Value**
Thermal conductivity (W/m-K)	41.5
Poisons Ratio	0.29
Density (kg/m^3)	8138
Machinability	Good
Hardness(Rockwell C)	65
Compressive yield strength (MPa)	3250

Elastic Modulus(GPa)	200

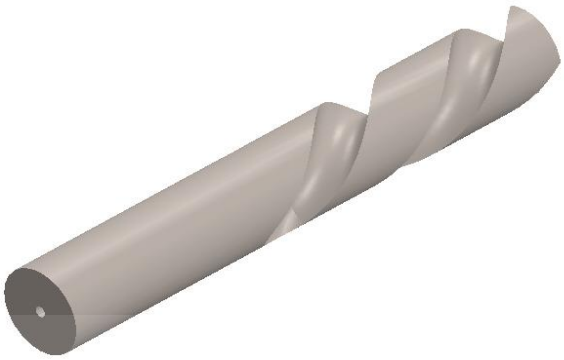

Figure 12: Thermosyphon Drill Bit

Figure 12 displays the thermosyphon drill bit that was tested. The drill was subjected to a thrust force of 353.868 N which was exerted on the chisel edge for a spindle speed of 420 rev/min. The friction torque acted on the flank face of the drill bit was 8.09 Nm for the speed of 420 rev/min.

The drill bit has a fixed boundary geometry condition that is applied to the drill bit shank, to replicate the drill environment on a drilling machine. In a drilling procedure the thrust force a nd torque is applied to the tip point of the drill bit where they serve as reaction forces.
Figure 13 represents a thrust force that is applied axially to the tip of the drill bit and this is in dicated by the purple arrows, then the torque is applied around the tip of the drill bit and rotates off the drill in the middle position and the yellow arrows demonstrate this.

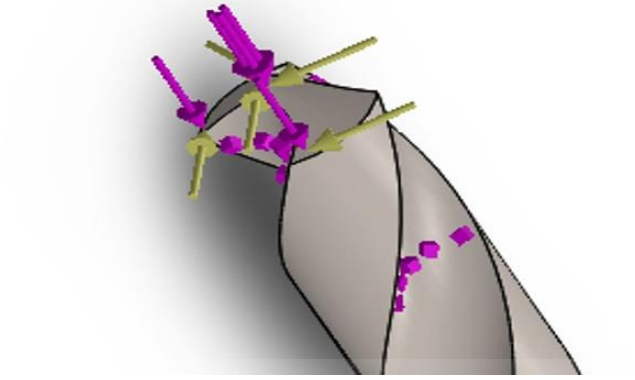

Figure 13: Drill Bit Loads

Boundary Conditions

Before the simulation occurs, the parts are subjected to boundary conditions. The simulation conditions to be applied are based on the thermosyphon drill bit's operating condition. During the drilling process, the thermosyphon drill bit is mounted onto the machine drill chuck or tool holder. The limiting condition to be applied on the thermosyphon drill bit is a fixed geometry, and this is denoted by green points as noted on Figure 14.

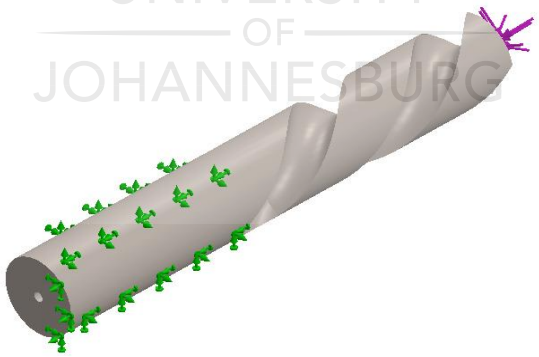

Figure 14: Drill Boundary Conditions

The maximum Von Misses Stress that is experienced by the drill bit is 15.69 MPa, where the total elements are 74020 and with 110745 nodes on a structural stress analysis. Figure 15 demonstrates the stress distribution within the drill bit and the maximum stress on the drill bit material.

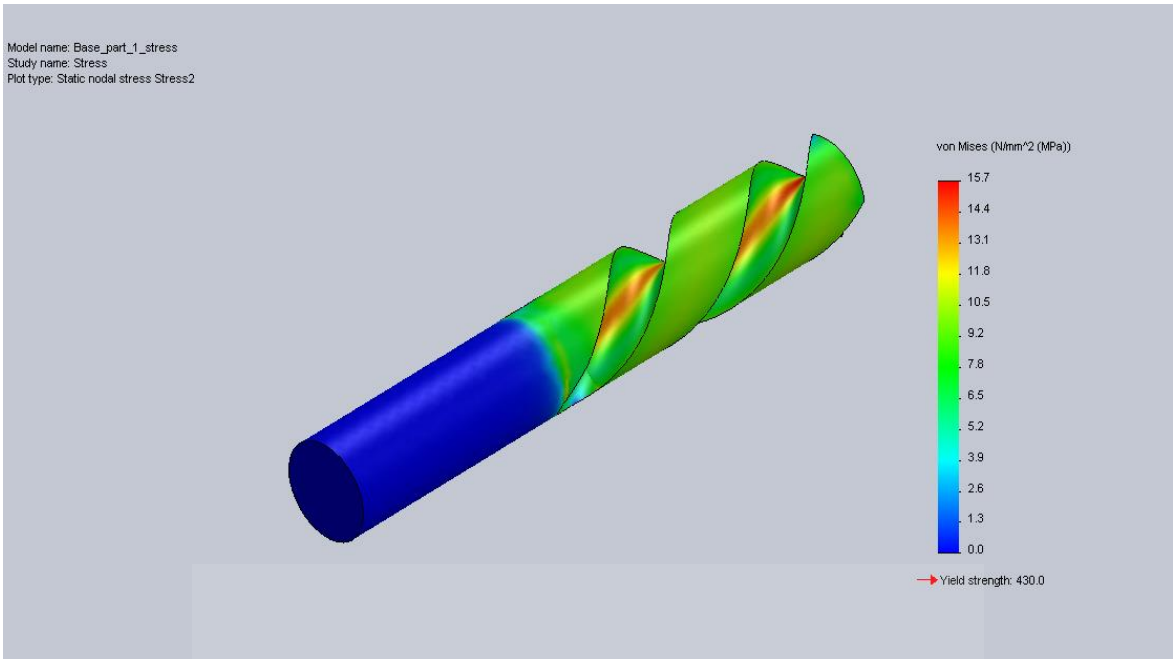

Figure 15: Drill Bit Max Von Misses Stress

The transient thermal analysis was also conducted on the drill bit as demonstrated on Figure 16. Except in the heating region, the drill bit has a fully insulated boundary condition applied to the whole drill. Heat is applied from the tip of the drill bit up to 25 mm on the drill bit flute. A heat load of 330 W was applied for 15 seconds on the drill bit cutting edge and along the flute to 25mm from the tip. Tharayil, *et al.* [60] conducted an experiment where they varied the load from 20 – 380W on the heat pipe, the authors also varied the filling ratios from 20%, 30% and 50%. This study considered the same loading on the drill bit for optimum heat transfer. The study by Jen, *et al.* [55] determined the optimal dimensions for the location of the thermosyphon depth within a drill. This study noted the heat application area which the authors determined to be 25 mm from the drill bit tip. Zhu, *et al*. [61] also considered an insertion of a heat pipe that is 32 mm away from drill bit tip for experimental purpose and the tip area was a heat application area. The maximum temperature experienced is at the tip of the drill bit at 457 ºC as depicted in Figure 16. This maximum temperature experienced reduces in the direction away from the drill tip along the flute.

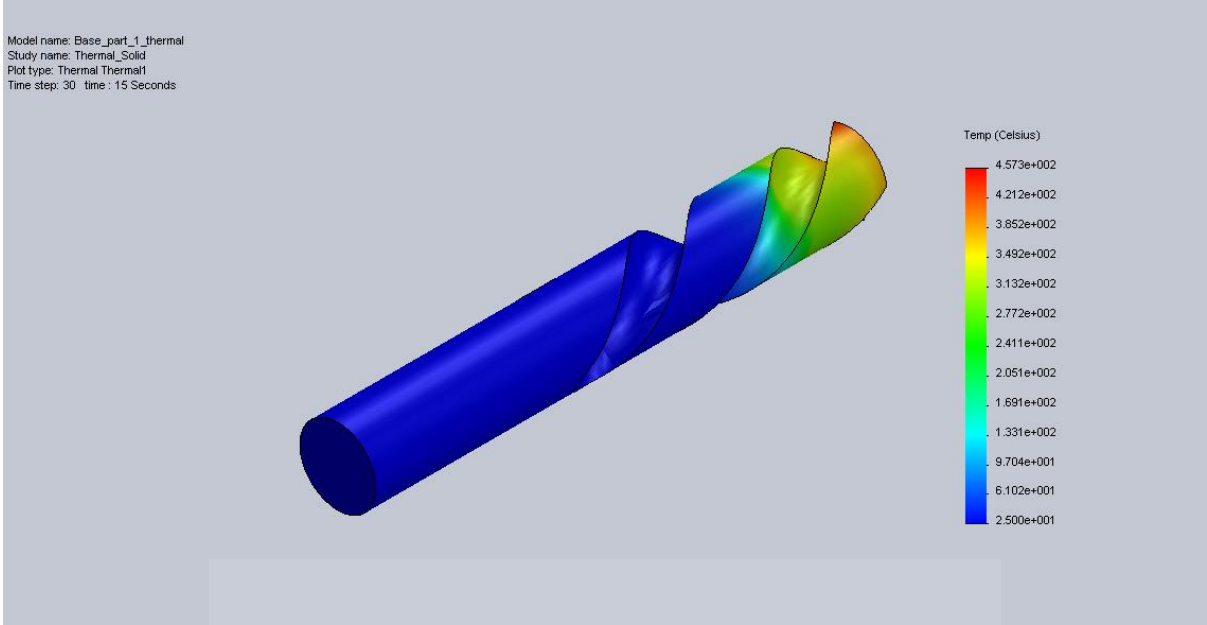

Figure 16: Drill Bit Max Temperature

A stress and thermal analysis conducted on Figures 15&16 was conducted on the drill bit tip as depicted on Figure 17. The drill bit tip experiences a temperature distribution from the maximum of 457 ºC maximum and down to a minimum of 250 ºC. The condition of the drill bit tip did not display signs of complete failure as depicted on the temperature distribution on Figure 16. The stress analysis was as expected along the web of the drill bit and along the wall as depicted on Figure 15.

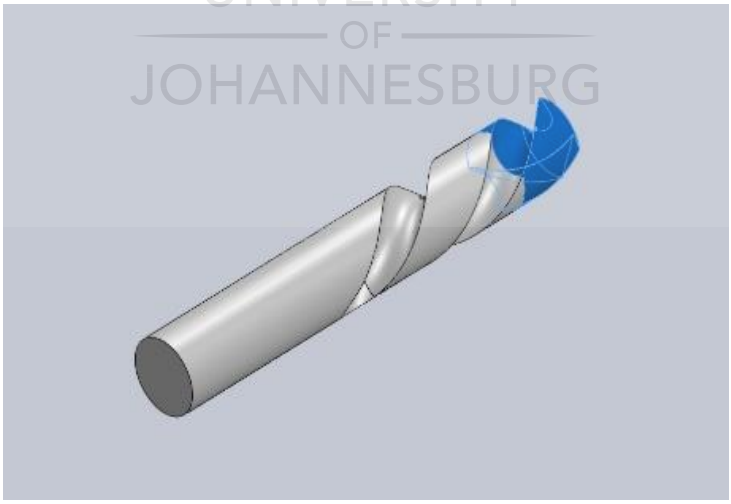

Figure 17: Drill Bit Tip Stress Point

3.4.3 Drill Bit Thermosyphon Taper

Jen, *et al.* [46] study considered optimal dimensions in the experimental study that was conducted for the use of a thermosyphon drill bit. The study was utilized as a guide in determining the optimal dimensions and location of the thermosyphon within the drill bit, due to the success that was achieved in the reduction of temperature of the drill bit tip. Figure 18 displays the taper thermosyphon inserted within the drill bit. The investigation conducted on the effect of rotational speed on a taper [4] supported the design of the insertion of a reverse tapered thermosyphon.

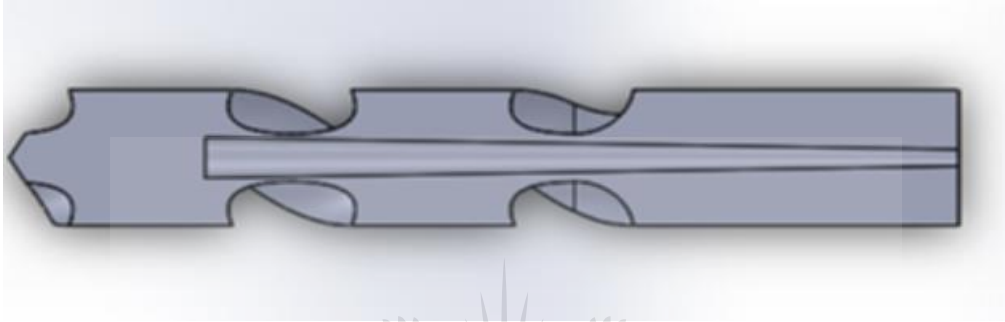

Figure 18: Taper Thermosyphon Drill Bit

The insertion of a reverse taper has been known to be of difficulty and as such there has been known little success of the insertion. This study did however note that the restriction of the drill bit web thickness will have to be considered and overall length of drill bit flute. According to Jen and Sequeira [4], the positioning of the thermosyphon within the drill bit has to be sufficient in order to ensure material integrity. The positioning of the thermosyphon within the drill bit has major advantages such a s prolonged tool life with the presence of the working fluid within the thermosyohon. Some of the advantages that this system present is the better hole dimensional control, lower cutting energy and the overall costs of machining when compared to previous drilling methods.

3.4.4 Drill Bit Stress Conditions for optimal length

The design parameters that will inform the design for best thermal performance while maintaining drill in position will be investigated.

The parameters to be investigated are the distance from the tip of the tool and the thermosiph on diameter, these will be calculated using stress simulations (to test the strength of the adjust ed drill) and thermal simulations (determine the thermosiphon drill bit performance). A number of FEA simulations were conducted as per Table 3 below. There were variations on the distance of the thermosyphon from the drill bit cutting edge from 5 mm up to 25 mm, which

is in line with the investigation by Jen, *et al.* [54]. Table 3 below displays that the highest stress is experienced closer to the drill bit tip and the stress reduces in the direction away from the drill bit tip.

Table 3: Thermosyphon Drill Bit Optimal Distance

Distance from Cutting Edge (mm)	Maximum Stress (MPa)	Maximum Temperature (ºC)
5	42.6546	292.962
10	39.2574	357.557
15	37.4413	400.954
20	36.6565	425.509
25	36.0825	440.147

The maximum temperature experienced on the drill bit tip, likewise is located 5 mm away from the cutting edge while the reduction in temperature is away from the cutting edge. The intersection of the two graphs of the maximum temperature and maximum stress are shown in Figure 19. This intersection of these two graphs shows the location of the optimal position of the thermosyphon from the cutting edge. This location is 12 mm and thus is a point where the larger diameter of the thermosyphon will be positioned.

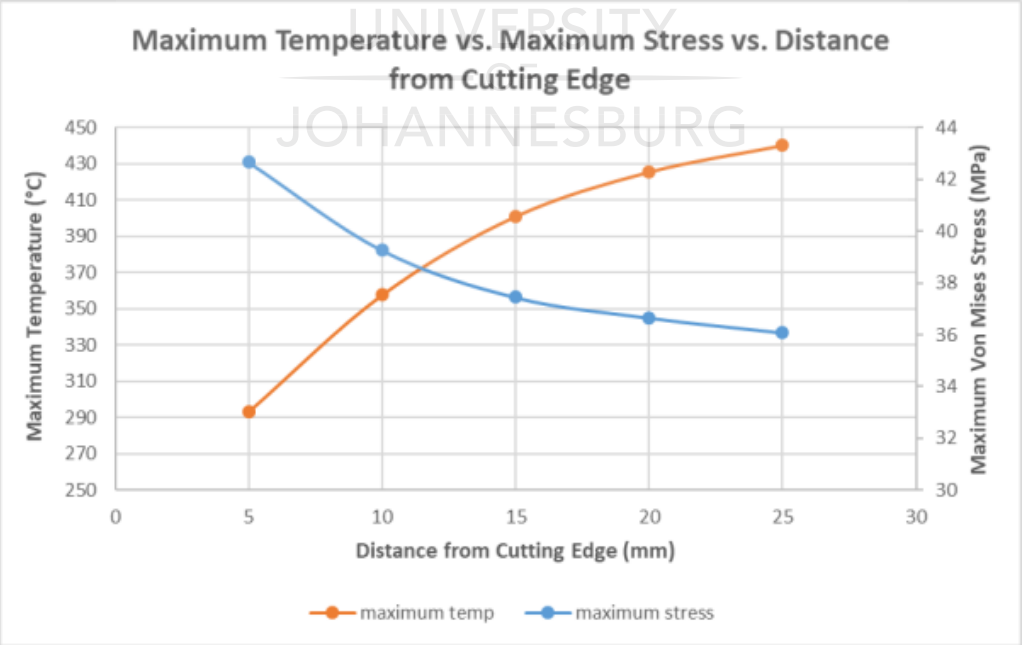

Figure 19: Maximum Temp vs Maximum Stress vs Distance from Cutting Edge

3.4.5 Drill Bit Thermal Conditions for optimal diameter

The determination of the optimal largest taper diameter of the thermosyphon was simulated similar to the distance from the cutting edge. The taper diameter was varied from 2 mm diameter up to 7 mm for the insertion within the restrictions of the drill bit web thickness. Table 3 demonstrates the stress and thermal analysis results for the varying taper diameters.

Table 3: Thermosyphon Drill Bit Optimal Diameter

Largest Taper Diameter (mm)	Maximum Stress (MPa)	Maximum Temperature (ºC)
2	15.7562	438.19
3	15.7585	436.13
4	16.5741	433.711
5	19.3813	431.942
6	27.0451	429.976

The variation of the taper diameter induces the stress for the largest based on the larger diameter, this is seen in table 3. The optimal taper diameter is therefore determined by the intersection of the two graphs of temperature and stress. The optimal largest diameter of the taper is 4.7 mm which is shown in Figure 20 where the two graphs intersect.

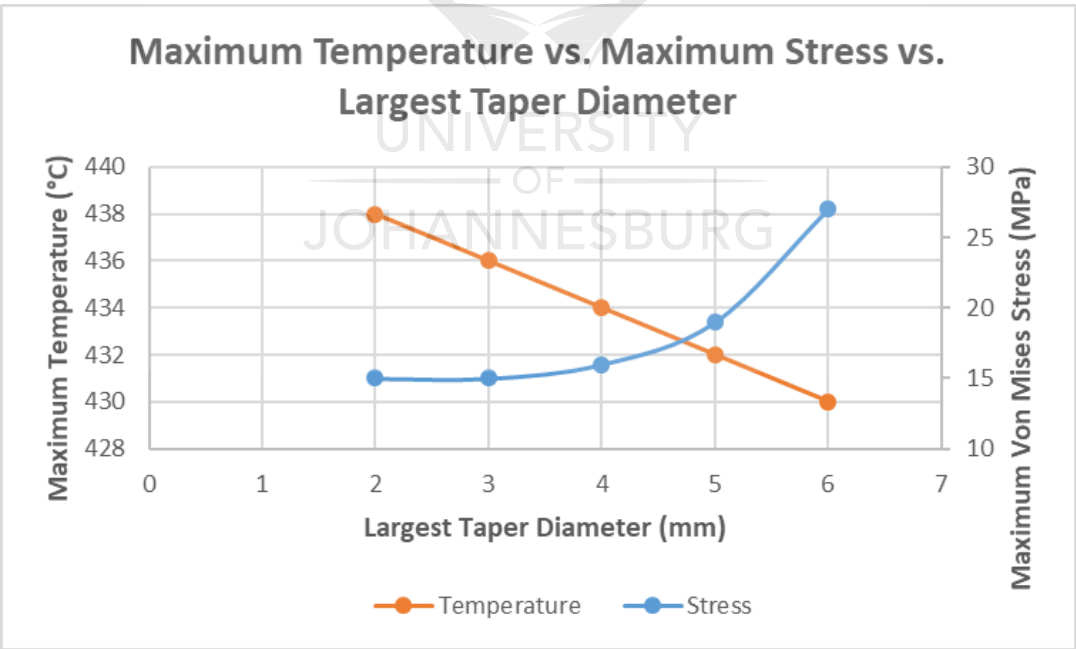

Figure 20: Maximum Temp vs Maximum Stress vs Largest Taper Diameter

A study by Jen, *et al.* [1] indicated a geometry that was limited to a parallel thermosyphon or parallel shaped for heat transfer. These studies have focused on a vertical drilling approach for the thermosyphon, due to the limitations of a parallel thermosyphon. The optimal positioning of the simulation for the largest taper and the distance from cutting edge have brought an

improvement in overcoming the limitations of vertical operation. The successful insertion of the taper thermosyphon within the drill bit overcomes the limitations described.

Geometry

Figure 21 displays the dimensions of the drill bit, for the reverse tapered thermosyphon tested. This study has considered the fact that Jen, *et al.* [1] were limited to a gravity assisted direction which did not consider a taper shaped thermosyphon. The optimal dimensions of the taper and distance from cutting edge were indications of the performance on a simulation. Jen, *et al*. [1] also utilized a long length drill bit at 266.7 mm thereby increasing the length of the shank. This study considered a shorter drill bit of 140 mm length sufficient for the optimal taper over the length of the drill bit. The drill bit consists of a truncated cone shaped thermosyphon with a 1º taper towards the top of the drill bit. The thermosyphon has a larger diameter at the bottom of the drill, located 25.4 mm away from the drill bit tip in order to ensure that the drill bit material does not weaken or fracture and is optimal for heat conduction as indicated by Jen, *et al.* [55]. The thermosyphon was thus optimized for a smaller diameter taper of 2.5 mm on a 140 mm overall drill bit length. The large taper was increased in order to improve the insertion on a larger web thickness beyond 6.5 mm. Jen, *et al.* [1] also recommended a larger thermosyphon diameter in order to ensure effective heat transfer. This study also opted for a reduced diameter of the drill bit in order to ensure that the use is of a parallel shank, therefore a 20 mm drill bit requirement is standard.

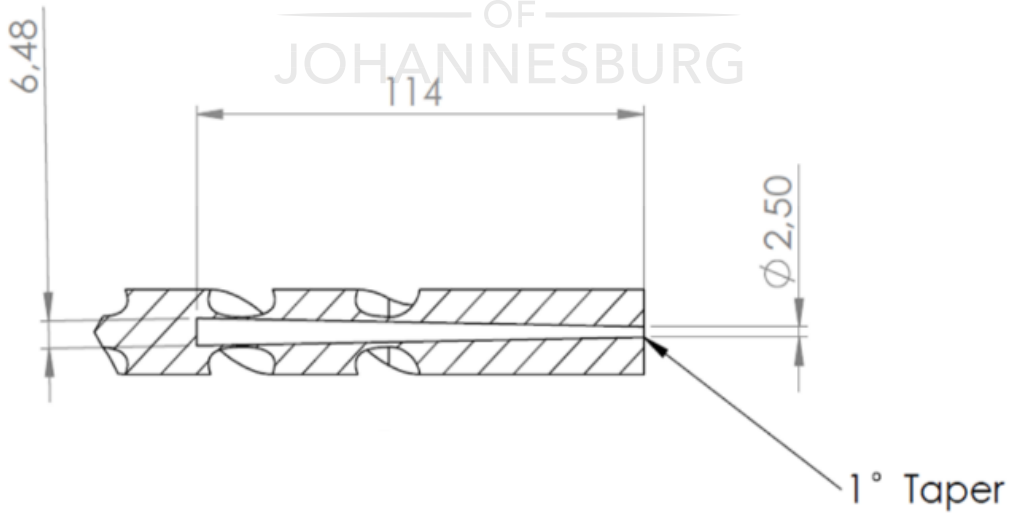

Figure 21: Thermosyphon Drill Dimensions

The improvement in the dimensions of the thermosyphon drill bit will overcome the limitations in vertical operation. This thermosyphon drill can therefore be tested using different orientations aside from the vertical.

Chapter 4: Manufacturing

4.1 Introduction

This chapter explains the manufacturing process of the drill bit to be utilized for the testing process that was carried out. This chapter will focus on the insertion of the reverse tapered thermosyphon within the drill bit, due to the complex nature of the process of insertion. The following manufacturing process on Figure 22 details the process flow chart for the manufacturing of the thermosyphon drill bit.

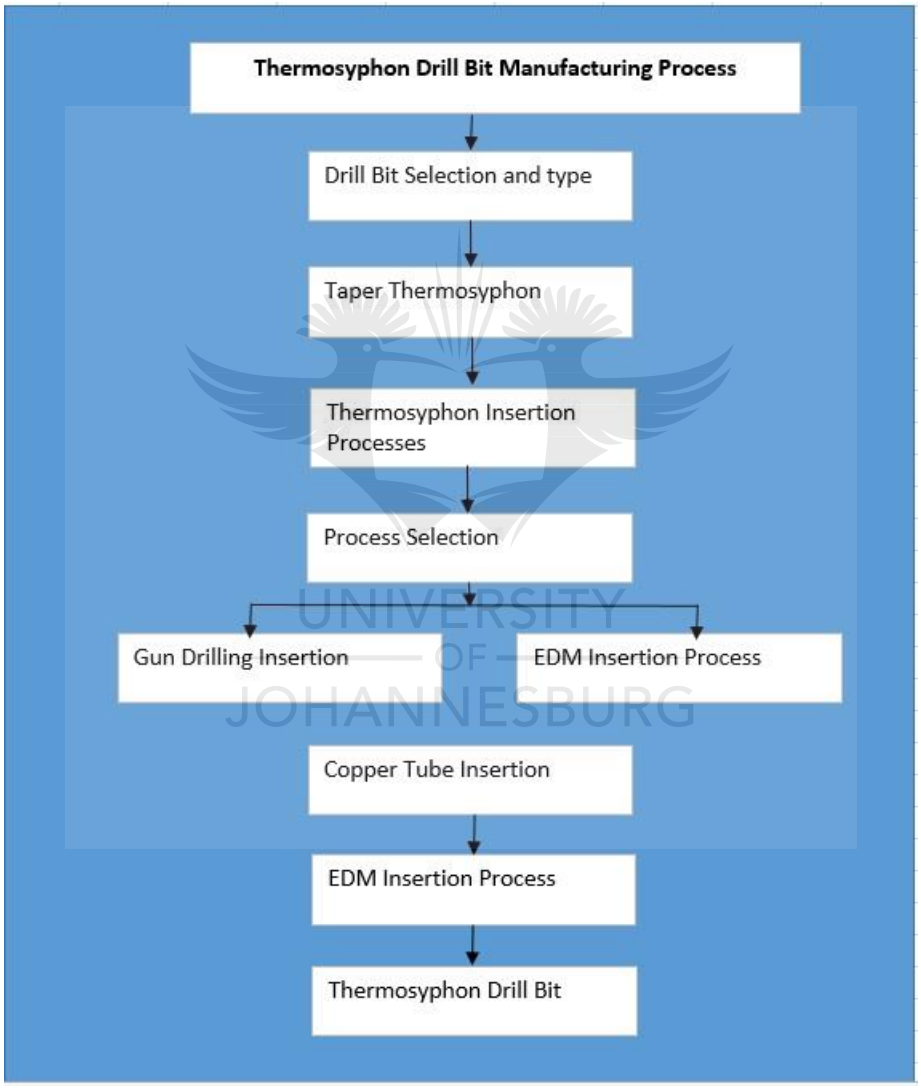

Figure 22: Thermosyphon Drill Bit Manufacturing Process

4.2 Drill Parameters

4.2.1 Drill Geometry and Material

The drill bit has been used broadly for the heat pipe and thermosyphon cooling through evaporation and condensation [1] [55] [62] [63]. The drill bit utilized on such studies have exhibited various type of drill bit dimensions. The most common used drill bit material has been the High Speed Steel material selection for experimental purposes and manufacturing. The drill bit selection utilized [62] was made of high speed steel and had the dimensions of 20 mm diameter and 254 mm in length of drill bit. This drill bit was used on an experiment where a heat pipe of dimensions 6.62 mm diameter and 222.6 mm in length was inserted within the drill bit. This type of drill was manufactured for a set of drill bits in order to carry out experiments for the solid drill bits and heat pipe drill bits. This study entailed the use of an armour piercing drill [64] of material high speed steel for the consistent testing.

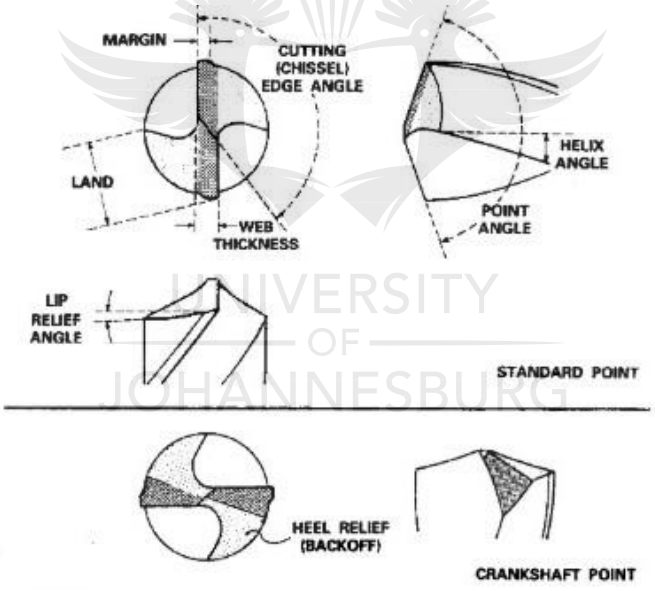

Figure 23: Drill web thickness[65]

The drill bit web thickness is designed to the limitations of the drill bit dimensions in length and diameter for standard drill types. Figure 23 shows the web thickness on the drill bit and the margin in relation to web thickness. The armour piercing drill has an advantage in the design of the web thickness on the drill bit due to the nature of the heavy duty type of drill bit [64]. This has therefore necessitated a large web thickness of 7 mm for standard armour piercing drills of high speed material. The web thickness and diameter of the drill of 20 mm as explained in Chapter 3 was selected to optimize the design requirements that were simulated. This

therefore ensured the feasibility of the insertion of a reverse tapered thermosyphon within the drill bit.

4.2.2 EDM Process Drilling

The thermosyphon insertion followed by the Electro-Discharged Machining (EDM) process of manufacturing. This process as explained was facilitated by the link in previous work conducted by the University of Johannesburg. The process is more expensive when compared to the gun drilling process but at this instant it offered a better solution for the insertion of the reverse tapered thermosyphon. The design of the AH-35 NA accutex EDM machine has limitations which have necessitated a consideration for manufacturing of the drill bit versus the design requirements. Figure 24 shows the EDM machine which was utilized for the thermosyphon cavity within the drill bit. The AH-35 NA Accutex machine has limitations in dimensions of the EDM electrode has an accuracy of Ra 0.18 µm surface finish of 50 mm thick material when using a 0.2 mm brass wire electrode[66].

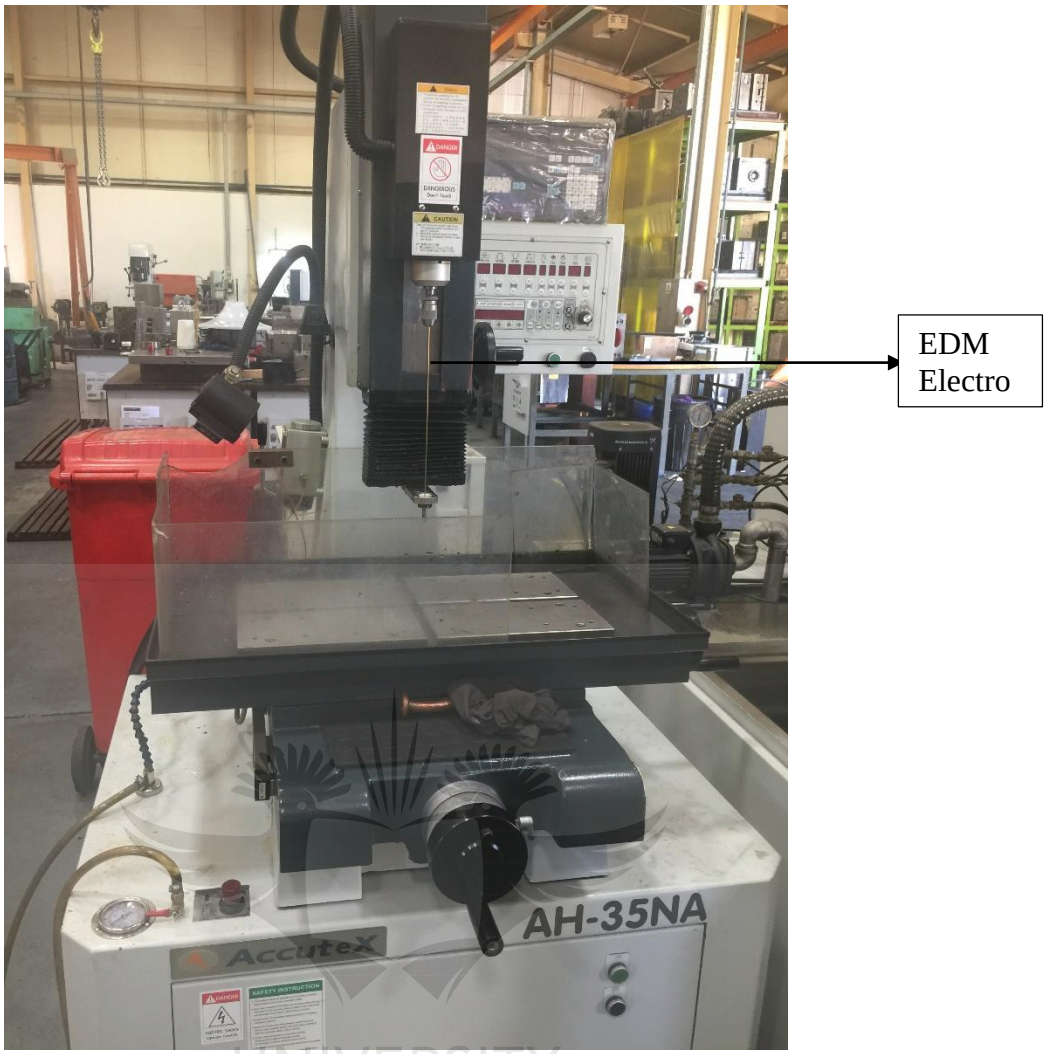

Figure 24: Drill web thickness

The EDM process followed ensured to remove particles through flushing process in order to maintain a consistent cavity of small holes [67]. This process as demonstrated on Figure 25 sought to advance a machined cavity for the insertion of a thermosyphon. The drill selection of armour piercing for heavy duty required a suited method of EDM processing for the creation of a cavity within a drill bit.

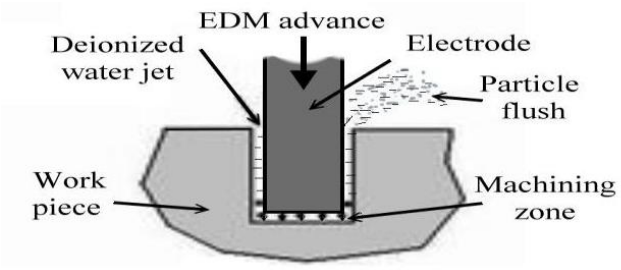

Figure 25: EDM fast drilling process [67]

The design requirements of the drill bit were of a reverse tapered cavity for the thermosyphon on 2.5 mm small diameter and 6.38 mm large diameter located 114 mm away from the drill bit tip. The use of the EDM process with the specification of the 0.2 mm brass wire electrode were limited to the 50 mm wall thickness in work piece material. This study considered an insertion which was 114 mm depth of material for a drill bit cavity and with such a requirement, the accutex machine was not capable to create such a reverse tapered requirement.

4.2.3 Drill Bit Cavity

The dimensions of the cavity within the drill bit are 5.012 mm in diameter, which complies to an H7 interference fit [68], for the insertion and 114 mm in depth as per the thermosyphon design explained in Chapter 2. Figure 26 displays the depth of the cavity in order to suit the design depth of the thermosyphon. This is also consistent with the amount of material that has to be left at the tip of the drill bit in order to ensure that the material integrity is intact as also explained in Chapter 2 and this is 25.4 mm from the drill bit tip.

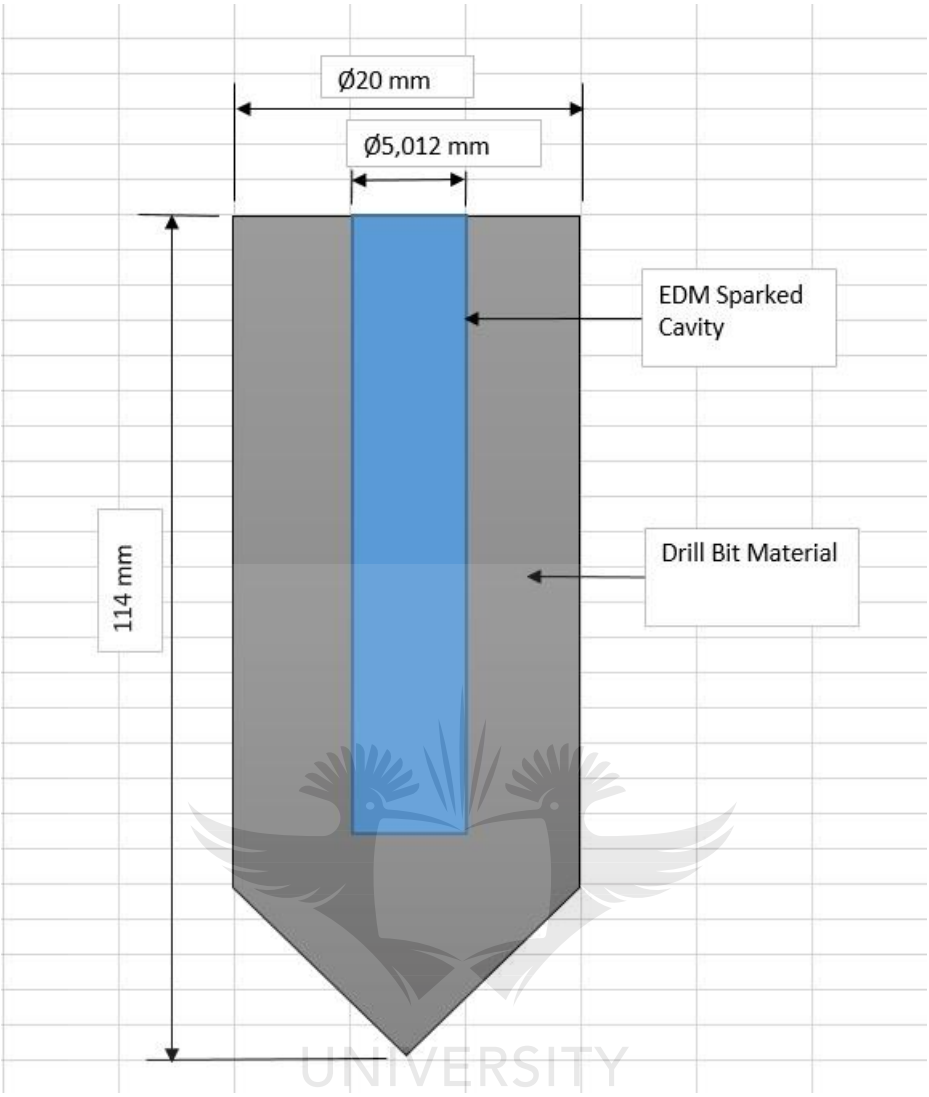

Figure 26: Drill Bit Sparked Cavity

4.2.3 Copper Tube Sparking

The copper tube entailed the use of a novel method for the insertion due to the complex nature of inserting a reverse tapered thermosyphon. This method sought to create a reverse taper within the drill tip without directly drilling the reverse taper within the drill bit. The complex requirement of the reverse tapered design discussed in Chapter 2 brought about a challenge that required a novel process. Figure 27 demonstrates the EDM sparked hole entailing the insertion of the copper tube reverse tapered with the large diameter of 5 mm and smaller diameter of 2.5 mm at the top of the drill bit. The process selected brought limitations due to the availability of specific sized electrodes to effect a 6.45 mm larger diameter hence the deviation to 5 mm. This newly selected dimensions also support the increase in the structural strength of the drill bit material due to the reduction in size but increase in wall thickness of web.

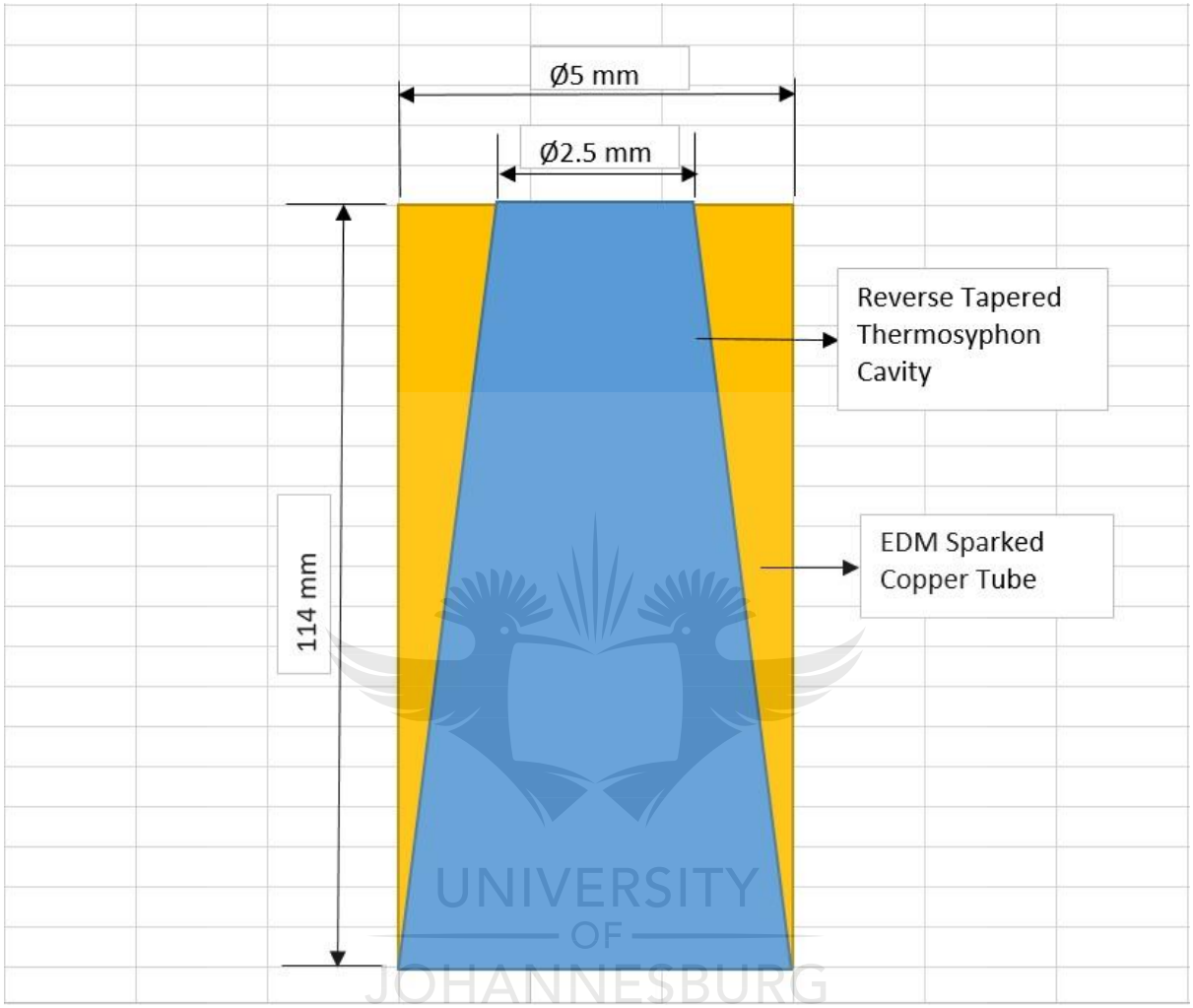

Figure 27: EDM sparked copper tube

The selection of the copper tube is due to the fact that it is a good conductor of heat, thermal conductivity (413 W/mK) [69], its water working fluid compatibility on heat transfer and as such has been consistently in use on heat pipe materials on previously manufactured [47].

Chapter 5: Testing

5.1 Introduction

This chapter will detail the process that has been followed, in carrying out the testing of three methods in drilling in order to determine the performance of the drill under varying conditions. The chapter will further detail the testing apparatus used, the equipment and the manner in which data was acquired. The test is carried out such that the heat is applied at the tip of the drill bit. This will be measured before entering the block of material to be drilled and on exit of the material drilled in order to determine the efficiency of the drilling method.

5.2 Testing Operation

The testing apparatus comprises of three testing specimens which are the drill bit that is cooled with metal working fluid, the drill bit that is utilized for dry drilling, not cooled with metal working fluid and the drill bit that has a reverse tapered thermosyphon. The apparatus of testing the effect of the thermosyphon on dry drilling operations will entail an insertion of a thermosyphon for effective evaporation and condensation. Jen and Sequeira [4], inspected the effect of rotational speed on the thermosyphon for cooling within drilling applications. They designed a tapered rig for experimental purposes and they determined that the rotational speed affected the flow of the fluid towards the large diameter of the taper. Figure 28 displays the test rig conducted.

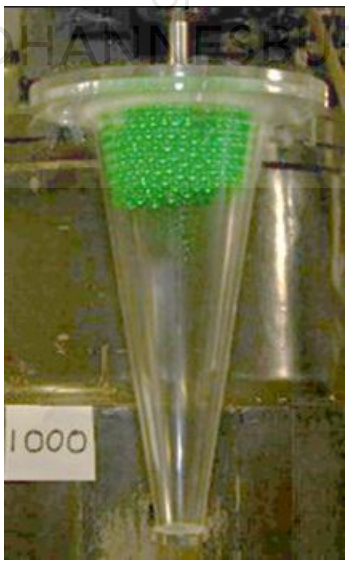

Figure 28: Tapered Thermosyphon Drill Rig Test [4]

This study has considered the test conducted by Jen and Sequeira [4], and noted the rotational effect of the working fluid within the tapered thermosyphon. The reverse taper effect will thus

ensure that a zero-net-gravity point of the thermosyphon working fluid is greater to prevent the boiler from drying out thereby affecting condensation and evaporation within the thermosyphon [4]. Figure 29 displays the flow of the working fluid of water and location within the thermosyphon drill bit. The heat flux input section is located at the largest taper position of the thermosyphon and this will be effected by the friction and drilling through the mild steel material. The heat flux output section where condensation will take place will be positioned on the smaller diameter of the taper.

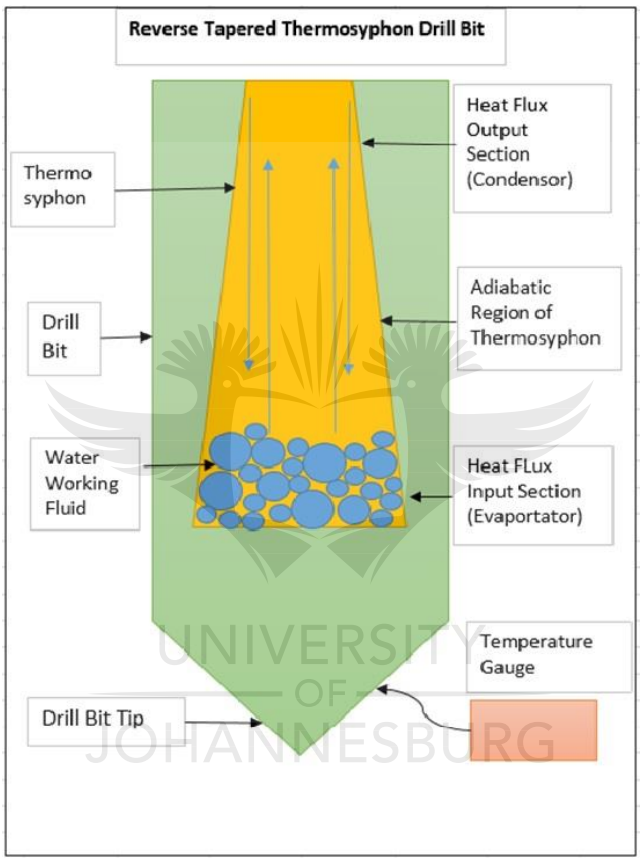

Figure 29: Reverse Tapered Thermosyphon Drill Bit

The use of the drill bit for the reduction of drill bit tip temperature was tested by Jen, et al. [1], where a parallel thermosyphon was inserted within a drill bit. Their study concluded on the limitations of the parallel thermosyphon that is limited to vertical operation, they further concluded that the limitation is therefore a disadvantage. Figure 29 represents the insertion of a reverse tapered thermosyphon within a drill bit for the reduction drill bit tip temperature. This testing process sought to overcome the limitations of vertical operations of thermosyphon drill bits.

5.3Testing Equipment

The drill bit on Figure 30 was driven on a radial arm drilling machine. This is to ensure that the drilling process is tested on a live environment. The drill bit was held on a chuck that is suitable to handle a 20 mm parallel shank drill bit. The workpiece was a mild steel plate that is 30mm in width in order to ascertain the process of heat flux application on the drill bit tip. Drilling through a 30 mm wide plate of mild steel will generate a heat flux within the drill bit tip which is similar to the simulated process explained in Chapter 3.

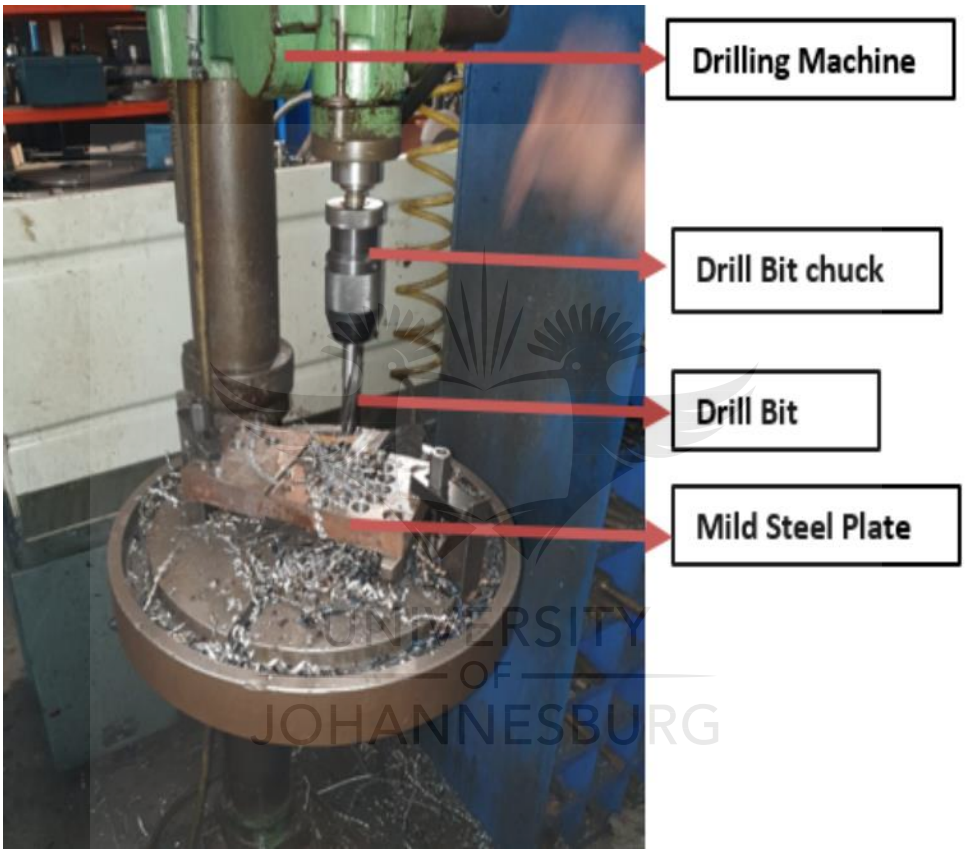

Figure 30: Drill bit on a radial drilling machine

The process of thermosyphon testing where the working fluid has to be contained within the drill bit is shown on Figure 31. The drill bit was heated for the pouring and containment of the working fluid within the drill bit. An Oxylasor torch was utilized for increasing the temperature of the drill bit to ~ 800 ℃, in order to remove the air within the thermosyphon tube.

Figure 31: Drill preparation and heating

Once the drill bit was heated up, and all vapor is removed from the thermosyphon tube, water was then quickly poured into the thermosyphon. Water working fluid to the amount of 3 ml was poured into the thermosyphon for the process of evaporation and condensation to take place. Water was inserted through the use of a syringe and needle due to the restrictions in dimensions of the entry hole. The thermosyphon entry top hole is 2.5 mm and as such presented a restriction in pouring water fluid within thermosyphon. Figure 32 shows the syringe and needle for reaching the depth of the thermosyphon. The depth of the thermosyphon is 114 mm from the top of the drill bit entry point and as such, a syringe alone could not ensure that water could reach the bottom of the thermosyphon. The use of the longer needle with a syringe ensured that the water working fluid is able to reach the bottom larger diameter of the thermosyphon.

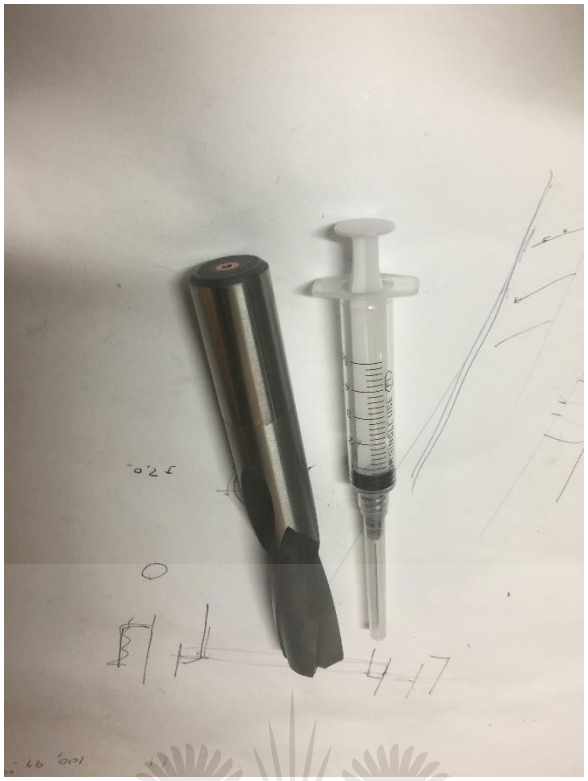

Figure 32: Needle for water working fluid

The thermosyphon was then sealed quickly with a steel pin for the containment of the working fluid as shown on Figure 33. The pin was knocked in with a hammer for quick locking and securing the top 2.5 mm entry point of the thermosyphon. A taper 10mm long steel pin was used with a diameter of 3 mm on a taper lead for easy entry.

Figure 33: Thermosyphon pin seal

The thermosyphon has to be sealed in order to contain the working fluid for ensuring process of evaporation and condensation. The infrared temperature gauge was used to determine the immediate temperature of the drill tip before entering and drilling through the block of mild steel. The infrared temperature gauge was also used to determine the exit temperature of the drill bit tip on exiting the block of mild steel.

Figure 34: Infrared Temperature Gauge

Figure 34 demonstrates the use of an infrared temperature gauge recording the temperature of the drill bit tip. This process was followed for the accurate measurement of the drill bit tip temperatures on entry and exit points. The infrared temperature gauge captured the temperature of the drill bit tip without interference of the metal chips. The measurements were conducted in such a manner that the entry and exit points of the drill bit were measured adequately without metal chip contact. The process was followed on three settings of the metal working fluid use, dry drilling and thermosyphon drilling.

5.5 Closing Remarks

The testing process was followed for the three sets of tests when using a solid drill bit without metal working fluid, solid drill for dry drilling and a thermosyphon drill bit without metal

working fluid. The evaporator section of the thermosyphon tested for the effect that it has on the drill bit tip on exit temperatures. The working fluid followed the evaporation process through the adiabatic section and condensation took place due to the restriction of the steel pin cap. This determined the effectiveness of the thermosyphon drill bit.

Chapter 6: Results and Discussion

6.1 Introduction

This chapter details the results obtained on the three sets of tests for drilling through the use of a solid drill without metal working fluid, drilling through the use of a solid drill with cooling of metal working fluid and the use of a thermosyphon drill without the use of a metal working fluid. The results will be demonstrated through the use of a tables for the number of holes drilled and graphical representation for the comparisons of the methods used.

6.2 Test Results

The testing method was conducted on a selected speed of 245 RPM for the three sets of drilling processes. The calculations of the drilling conditions were conducted for the three sets of tests carried out in Appendix A:

At 245 rev/min:

The cutting speed is calculated as 15.3938 m/min.

The feed is calculated as 6.223 mm/min.

The feed force is calculated as 448.043 N.

The torque is calculated as 4.9 Nm.

6.2.1 Dry Drilling

The test involved the use of an armour piercing drill [64]. The drill has the suitability of a large web thickness for the successful insertion of a taper thermosyphon within a drill bit. Chapter 3 detailed the requirements of the reverse tapered thermosyphon suitable for a 2.5 mm small diameter hole and 6.38 mm large diameter taper. The selection of the drill type ensured the insertion the fit of the large diameter as the web thickness of the armour piercing drill is 7 mm when compared to standard drill bits of 3 mm web thickness [64]. The drill was modified from the taper shank in order to maintain a standard parallel shank as detailed in Chapter 4. The parallel shank maintained a 20 mm diameter drill for the radial drilling machining as opposed to the requirements of a morse tapered shank. The parallel shank involved the use of a drill bit chuck suitable to drive a parallel shank.

The speed that has been selected is 245 rpm for the dry drilling, metal working fluid drilling and thermosyphon drilling. This selection has taken into consideration where Jen and Chen,

[63] conclude that the effect of rotational speed has a negligible effect in the temperature differences. The rotational speed selection has not had adverse effects on the comparisons for the temperatures of heat pipes. The selection of the 245 rpm sought to test the capability of the reverse tapered thermosyphon drill bit for wicking away heat from the drill bit tip. There were three drilling operations that were carried out on a block of mild steel plate. A series of 37 holes were drilled on the mild steel block in order to determine the temperature changes over the drilling of the holes. The numbers were selected due to the dimensions (20 mm diameter holes) of the available blocks of mild steel for drilling tests.

The results on Table 4 shows the drill bit temperatures that were experienced when drilling through the block of steel. The temperatures were measured by the Infrared Temperature gauge in order to determine the drill bit tip entry and exit temperatures upon starting and completing the drill activities. The temperatures were measured immediately before entry of the drill bit tip on the edge by the infrared temperature gauge and immediately on exit of the drill bit tip, the temperature was also gauged to ensure that there is no time difference which could influence the outcome.

Table 4: Dry Drilling at 245 rpm

Dry drilling at 245 rpm			
No of Holes	**Drill Tip Temp Before (°C)**	**Drill Tip Temp After (°C)**	**Duration (sec)**
1	18	126	70
2	44	157	73
3	47.9	142	78
4	50.5	137.5	78
5	61.9	182.4	85
6	63	156	85
7	67	196	71
8	71	152	77
9	73	192	79
10	69	173	88
11	72	186	82
12	83	196	70
13	84.9	190	69
14	81.5	203.7	80
15	82.9	215	75
16	80	194	78
17	78	229	74
18	86	215	75
19	83	223	76

20	89	232	77
21	91	227	75
22	89	226	70
23	96	274	75
24	88	215	77
25	84	239	79
26	90	222	80
27	96	238	77
28	97	247	72
29	98	230	70
30	103	212	75
31	107	228	78
32	109	249	71
33	110	258	75
34	123	275	70
35	147	309.3	79
36	174	333	74
37	224	421	70

These results show the sturdy increase of the drill bit tip temperatures on exit of the drill bit from the mild steel block. The temperatures indicate the performance of the solid drill bit without the use of metal working fluid for cooling the drill bit tip. The drill experiences high temperatures due to no form of cooling on the continuous entry and exit of the mild steel block of material. The following Figure 35 demonstrates a graphical representation of the results that have been experienced on dry drilling.

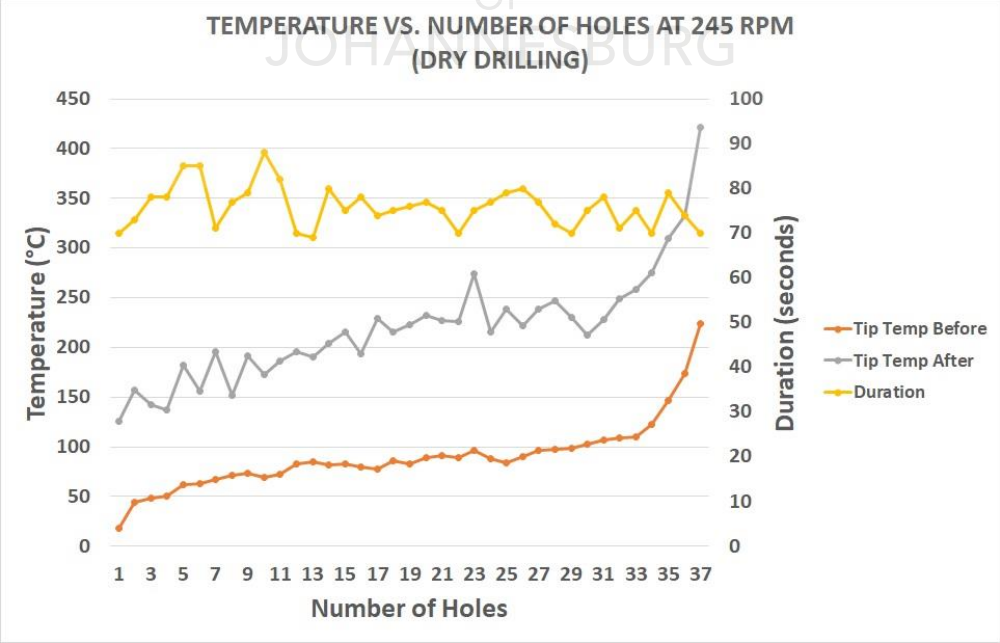

Figure 35: Temperature vs Number of Holes at 245 rpm

The use of metal working fluid alleviates the heat from the drill bit containment within the material being drilled, the high temperatures experienced as seen on hole 36 in Table 4 were also experienced by Zhu, *et al.* [70], the maximum temperature experienced was 343.1 ℃ in such a case. The graph in Figure 35 shows a trend in the temperature changes, this further displays the steep change in solid drill temperature from hole 26 where the temperature starts off at 222 ℃. The sharp increase passes the previous maximum temperature of 343.1 ℃ experienced by Zhu, *et al.* [70] in heat pipe cooling and thus continues to reach a peak of 421 ℃. The drill was adversely affected upon the drilling of 37 holes, and this can be seen based on the condition of the drill bit tip flank wear. Figure 36 depicts the condition of the drill bit tip flank wear and edges.

Figure 36: Dry drilling drill bit failure

6.2.2 Metal Working Fluid Drilling

Table 5 displays the results of the use of metal working fluid to cool the drill bit tip on the solid drill. The results were carried out for a number of 37 holes which is consistent to the dry drilling test done. The performance of the solid drill bit in the use of metal working fluid is expected

to exhibit low temperature increases hence the emphases is rather on the two processes of dry drilling and thermosyphon drilling.

Table 5: Metal working fluid drilling at 245 rpm

Metal working fluid drilling at 245 rpm			
No of Holes	**Drill Tip Temp Before (°C)**	**Drill Tip Temp After (°C)**	**Duration (sec)**
1	27	57	75
2	48	56	65
3	47	62	67
4	49	52	68
5	44	59	65
6	49	60	70
7	48	67	75
8	51	62	63
9	53	63	75
10	55	62	74
11	58	68	78
12	54	66	76
13	56	67	78
14	52	65	81
15	55	66	75
16	54	65	78
17	60	66	79
18	58	65	75
19	55	62	73
20	56	61	78
21	59	67	73
22	54	65	78
23	60	69	79
24	62	68	74
25	59	69	74
26	61	70	73
27	55	63	76
28	54	66	74
29	57	67	71
30	55	67	75
31	56	69	75
32	57	68	76
33	59	69	79
34	54	65	78
35	61	68	79
36	58	67	72
37	60	69	75

The results following are also displayed graphically in order to demonstrate the performance of the drill bit when using metal working fluid to cool the drill bit. The graph on Figure 37 displays the performance of the drill bit.

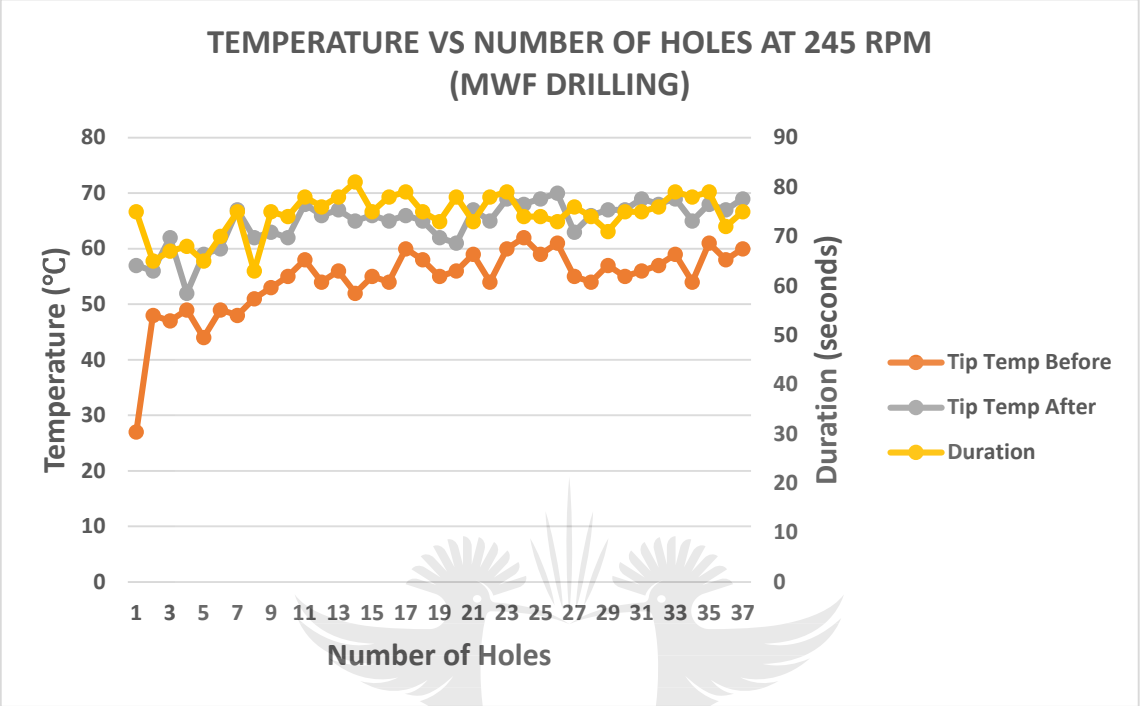

Figure37: Temperature vs Number of holes at 254 rpm

The drill bit cooling with metal working fluid experiences a steady temperature average increase between the entry and exit temperatures. The temperatures do not have a drastic increase due to the cooling effect of metal working fluid. The maximum temperature reached can be seen on the 26th hole to be 70 ℃ which is consistent to the effect of metal working fluid as expanded upon in Chapter 2. This is where it is explained that one of the functions of metal working fluid within machining applications is to remove heat away from the friction points and it is thus evident on the 70 ℃ maximum exit temperature.

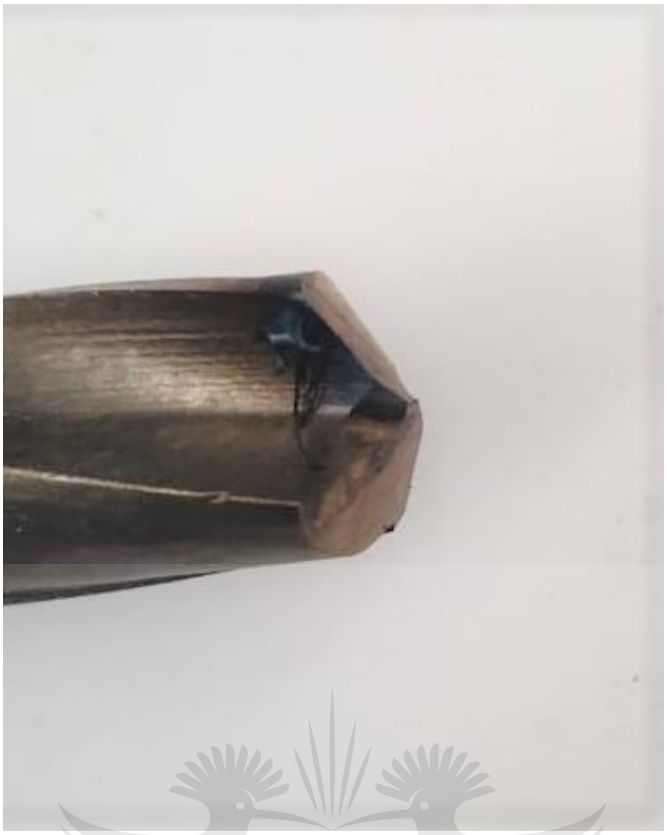

Figure 38: Metal working fluid drill bit tip

The condition of the drill on Figure 38 shows that the drill bit flank has not exhibited wear due to the effect of metal working fluid. The fluid has managed to remove heat away from the drill bit tip, but as explained in Chapter 2, the harmful effects of metal working fluid cannot be stressed more. The study has thus sought to implement a solution to avert the harmful effects of metal working fluid.

6.2.3 Thermosyphon Drilling

The results on Table 6 show the performance of the reverse tapered thermosyphon drill bit. This drill bit, was set for drilling a series of 37 holes similar to the dry drilling activity. This particular drill bit with the insertion of a reverse tapered thermosyphon, is compared to the solid drill and metal working fluid methods.

Table 6: Thermosyphon drilling at 245 rpm

Thermosyphon drilling at 245 rpm			
No of Holes	**Drill Tip Temp Before (℃)**	**Drill Tip Temp After (℃)**	**Duration**
1	17	146	85
2	30	160	89

3	52.4	201	85
4	59	199	86
5	67	214	89
6	68	189	87
7	70	198	86
8	87	205	89
9	83	211	85
10	87	190	79
11	89	190	80
12	92	185	85
13	89	198	87
14	87	209	85
15	95	210	84
16	98	234	89
17	103	228	88
18	105	214	84
19	126	229	83
20	93	224	89
21	84	219	87
22	89	270	78
23	129	257	81
24	133	236	85
25	126	233	89
26	120	240	84
27	96	229	83
28	92	214	85
29	95	261	79
30	99	241	75
31	138	232	78
32	132	256	80
33	104	238	79
34	136	254	85
35	141	249	89
36	120	250	88
37	149	251	80

The following results demonstrate the graphical representation of the reverse tapered thermosyphon. Figure 39 demonstrates the steady increase in the exit temperature when compared to the entry temperatures. The exit temperatures peak at hole number 23 where the exit temperature is 270 ℃. This is lower compared to the solid drill on dry drilling where the exit peak temperature was 421℃. The heat pipe has a wicking away capability of 30-50% when used in a drill containment, compared to dry drilling method [55]. The 421℃ maximum exit temperature result of the solid drill on dry drilling method when compared to the maximum

exit temperature of 270 ℃ for thermosyphon inserted within the drill is consistent with the results obtained on a study by Jen, *et al.* [54].

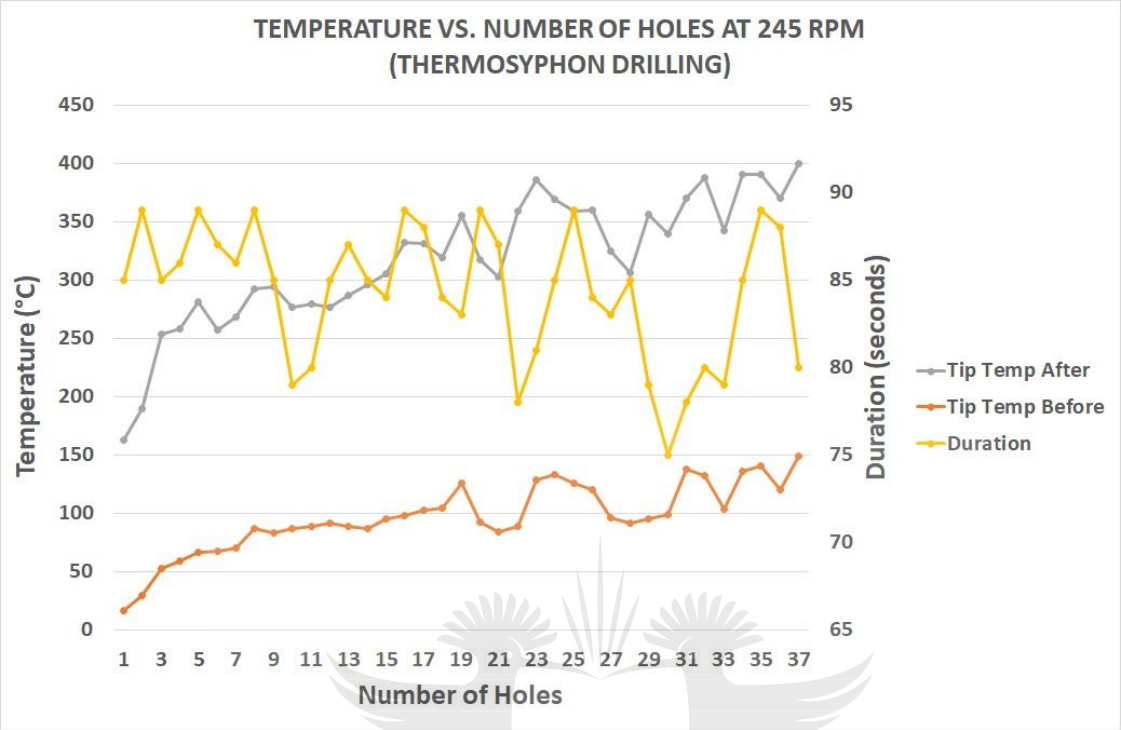

Figure 39: Temperature vs Number of Holes at 245 rpm

Figure 40 demonstrates the condition of the thermosyphon after drilling the 37 holes similar to the dry drilling method. The drill demonstrated signs of failure but not as adverse as the conditions demonstrated on the dry drilling method. The condition of the thermosyphon displayed signs of built up edge on the drill bit edges. High tool temperatures are often experienced at the tip of the tool and as such promote build up edge [63]. The initial signs of the thermosyphon drill seemed to suggest built up edge but the assessment was later conducted in order to ascertain the condition of the drill bit tip.

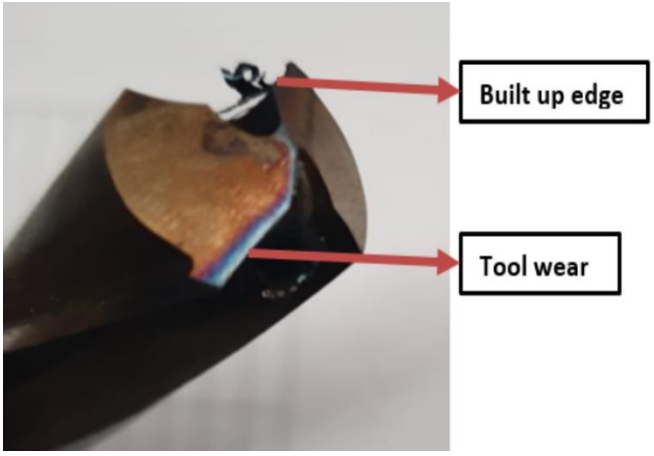

Figure 40: Thermosyphon drill with tool wear

The condition of the thermosyphon drill bit swarf was analysed in order to ascertain the extent of the drill bit wear. Figure 41 demonstrates close upon the condition of the drill bit cutting edge on a micro scope. Build up edge has to be measured to determine the flank wear and as such, when it is in excess of the value 0.1 mm, it is normally considered severe [1]. Judging by the condition of the cutting edges, on a 200 µm scale, on Figure 41, it is evident that the thermosyphon tool life is better than that on a solid drill bit.

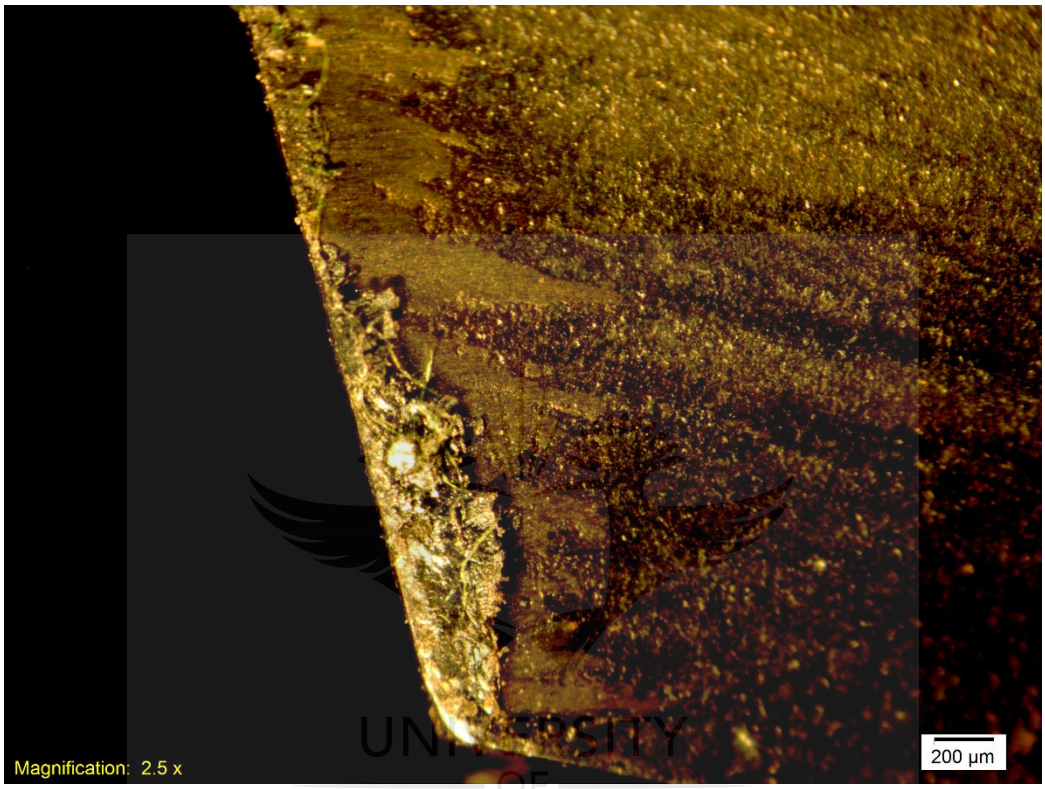

Figure 41: Thermosyphon Drill Bit after drilling

Figure 42 shows the condition of a new drill bit that had not been utilized for the comparison to that of a thermosyphon drill after a drilling activity. The results show that cutting tool life has not been severely affected after drilling 37 holes on a thermosyphon drill.

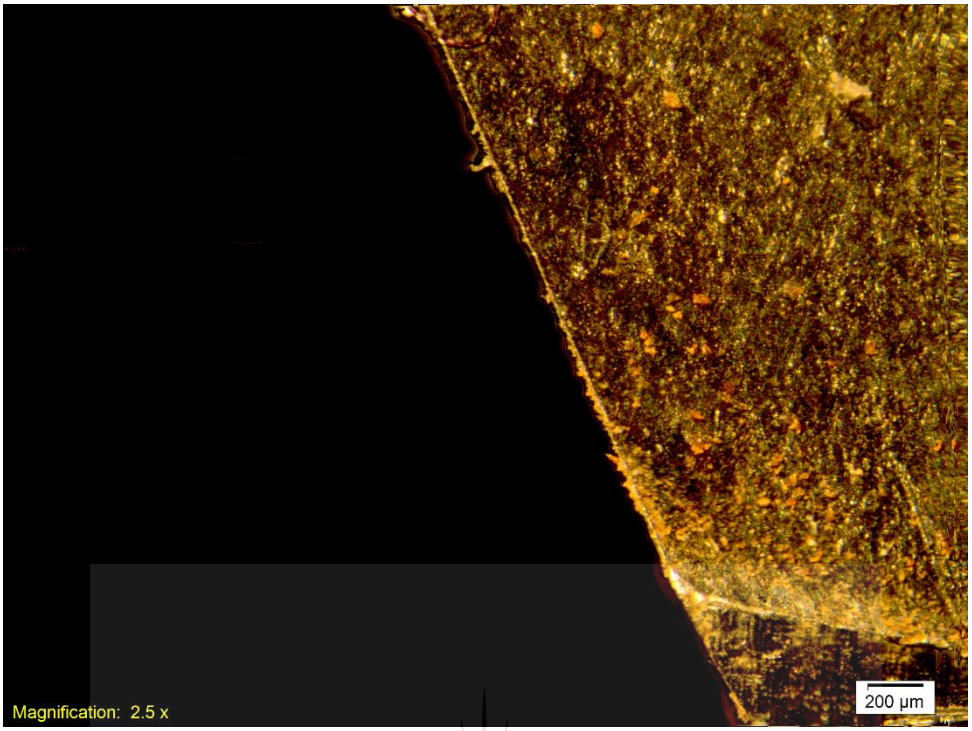

Figure 42: New Drill Bit

Adhesion of work piece material to the drill bit cutting edges was also found on the cutting edge. This is consistent to what Zhu *et al.* [61] when conducting experiments using heat pipe embedded drills. The solid drill demonstrated failure when going through the work piece material and as such severe adhesion of the swarf material on the drill bit cutting edges can be seen on Figure 43.

Figure 43: Solid Drill Bit after drilling

6.3 Boiling Limit Analysis

The dimensions of the thermosyphon as depicted in Figure 19 detail an overall length of 114 mm with a 1˚taper over the length of the thermosyphon. The volume of the thermosyphon on a truncated cone shape is [71]:

$$V = \frac{1}{3} \times \pi \times h \times (r^2 + r \times R + R^2) \qquad (6.1)$$

Where;

R = Base radius (mm)

r = Top radius (mm)

h = Height (mm)

V = Volume (mm^3)

$$V = \frac{\pi \times 114(3.24^2 + 3.24 \times 1.25 + 1.25^2)}{3}$$

$$= 1.923 \text{ mm}^3$$

$$= 1.923 \text{ ml}$$

Sequeira and Jen, [4] considered the correlations of the boiling limit by Faghri, [42] and the boiling limit by Sunt and Lienhardj, [72]. The entrainment limit was modified such that it contained the effective gravity for a rotating tapered thermosyphon. The boiling limit for the rotating tapered thermosyphon was thus determined as [4]:

$$q_T(r) = 0.149\rho_v h_{fg}\left(\frac{\omega^2 r\sigma[\rho_f - \rho_v]}{{\rho_v}^2}\right)^{\frac{1}{4}} \qquad (6.2)$$

Where:

q_T = Critical heat flux (boiling limit) (W/m^2)

r = Radial position (m)

h_{fg} = Latent heat of vaporization (kJ/kg)

ω = Rotational speed (rad/s)

σ = Surface tension (N/m)

ρ_l = Saturated liquid density (kg/m^3)

ρ_v = Saturated vapor density (kg/m^3)

The values are obtained from the thermophysical properties of saturated water table [73].

Analyzing the boiling limit:

$$q_T(r) = 0.149\rho_v h_{fg}\left(\frac{\omega^2 r\sigma\left[\rho_f - \rho_v\right]}{{\rho_v}^2}\right)^{\frac{1}{4}}$$

$$= 0.149 \times 0.59559 \times 2257\left(\frac{25.6563^2 \times 0.01 \times 0.0589\,[996.92 - 0.59559]}{0.59559^2}\right)^{\frac{1}{4}}$$

$$= 1150.58\ \text{kW/m}^2$$

Calculation for the energy partition on the tool face:

Converting the rotational speed [74]:

$$\omega = \frac{2\,\pi\,N}{60} \tag{6.3}$$

Where:

ω = Rotational speed (rad/s)

N = Rotational speed (rev/m)

Substituting the values;

$$\omega = \frac{2\,\pi \times 245}{60}$$

$$= 25.656\ \text{rad/s}$$

Calculating the cutting speed [75]:

$$V = \omega\, r \tag{6.4}$$

Where:

V = Cutting speed (m/min)

r = Radius (m)

Where the radius is found from the Ø20 mm drill bit in use.

Substituting the values;

$$V = 25.656 \times 0.01$$

$$= 0.25656\ \text{m/s}$$

$$= 15.3936\ \text{m/min}$$

The total shear force on the cutting tool face and metal chip is [76];

$$F_{fr} = F_v \sin\gamma + F_s \cos\gamma \tag{6.5}$$

Where:

F_{fr} = Total shear/friction force (N)

F_v = Tangential cutting force (N)

F_s = Feed force (N)

γ = Rake angle (◦)

Substituting the values;

$$F_{fr} = 448.043 \sin 15 + 10.4762 \cos 15$$

$$= 126.07 \text{ N}$$

The total friction energy on the interfacing of the cutting tool and metal chip that will be dissipated is [77] ;

$$q_2 = \frac{F_c V_c}{Jab} \quad (6.6)$$

Where:

F_c = Friction force (N)

V_c = Cutting Speed (m/s)

J = Mechanical equivalent of heat

a = Length of contact between cutting tool and metal chip (mm)

The length of contact is found on the drill bit point angle of 130̊ where the length is on the radial blade [78];

$$a = \frac{10}{\sin 65} \quad (6.7)$$

$$= 11.03378 \text{ mm}$$

b = Width of the chip (mm)

Substituting the values;

$$q_2 = \frac{126.07 \times 0.25656}{1 \times 0.011 \times 0.004}$$

$$= 735.102 \text{ kW/m}^2$$

The heat that is per unit time per unit area is signified by (1- R_2) q_2 and this is where the cutting tool and the workpiece intersect for metal chip formation [77].

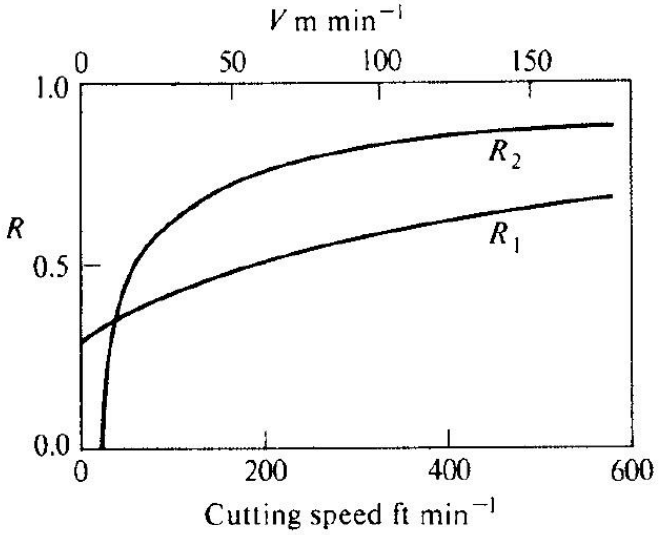

Figure 44: Variation of R_1 and R_2 for data [77]

R is found from figure 44, based on the cutting speed that is calculated to be 15.3936 m/min. The percentage estimation of R_2 is worked out to be 50 %.

The total heat from the tool and chip interface is [77];

$$q_T = (1 - R_2)\, q_2 \tag{6.8}$$

Where:

R_2 = Variation of factor

q_2 = Heat on tool face interface (W/m^2)

Substituting the values;

$$q_T = (1 - 0.5)\, 735102.7$$
$$= 367.55 \text{ kW/m}^2$$

936.4 Closing Remarks

The three tests that were conducted displayed characteristics of wear but to varying degrees upon the results displayed The solid drill was heavily affected in comparison to the thermosyphon drill on drilling through the work piece material. The following Chapter will conclude on the results that were obtained from the three tests that have been conducted.

Chapter 7: Conclusion

8.1 General Remarks

This chapter will provide and summary of the findings that were obtained during the experimental research process and will address these findings critically. This chapter also addresses the observed challenges, problematic areas and recommendations for further research.

8.2Overview of results

The three sets of results are for the methods of dry drilling, metal working fluid and thermosyphon drilling and this being similar to previous research. The tests conducted yielded results of better thermal management properties of the thermosyphon drill bit when compared to the metal working fluid and dry drilling processes. This study introduced an improvement through exhibiting better thermal management abilities. The large diameter of the thermosyphon contained the water working fluid for longer periods, thereby averting boiler dry out which could have limited efficiency of the evaporation and condensation process. The condition of the dry drilling process drill bit was severely affected as demonstrated on Figure 33 due to the absence of metal working fluid and this drill is not the thermosyphon type. working fluid and metal working fluid. The thermosyphon drill bit condition after completing drilling the same number of holes as the dry drilling was on a better condition. This drill in fact could continue drilling more holes since the drill bit cutting edges were not severely damaged.

The metal working fluid drilling process has always been expected that the results will be that of a drill bit that is not damaged due to the impact of metal working fluid. The metal working fluid removed heat from the cutting zone and also cleared off swarf in order to improve cutting tool life. This therefore ensured that the drill bit condition is such that it could drill even more holes, the fact however needs to be noted that the environmental effects and harmful effects of metal working fluids towards employees are the reason for this study. The drastic change in temperatures after drilling when using the dry drilling process peaking at 421ºC when compared to the thermosyphon process at 251ºC. The evaporation and condensation process was optimized through the use of the reverse tapered thermosyphon.

This was also proved on previous work done where the authors investigated the induction of an acceleration of the working fluid due to the rotating action of the reverse tapered thermosyphon, this has thus been seen on this study. The high temperatures experienced in the

thermosyphon and dry drilling process are attributed to the friction between the drill and mild steel material when the materials are in contact and in rotation. High temperatures have been experienced in the past when there were comparisons to the metal working fluid drilling process. The improvement in web thickness of 7 mm of the high speed steel drill bit in this study ensured the successful insertion of the reverse tapered thermosyphon. The improvement in web thickness is a need due to the challenges of a smaller web thickness. This study has demonstrated the effectiveness of the evaporation and condensation process.

8.3 Suggestions for further work

This study focused on the insertion of the thermosyphon using the method of EDM, the EDM process was efficient in creating a cavity within the drill bit. This study however did not focus on the gun drilling process when creating a cavity. There is therefore a recommendation to consider creating a cavity using a gun drilling method due to the ability of the gun drilling process to use smaller drill bits. Previous studies also used the gun drilling method for the parallel cavity within the drill bit for inserting a thermosyphon. The gun drilling process could be compared to the EDM process that was utilized in this study in order to gauge the efficiencies in the two methods for their abilities on a reverse tapered thermosyphon.

The test was conducted within a selection in speeds of 245 rpm, it is recommended that a variation in drill speeds and feeds should be conducted for further studies. The current results have shown the capacity of the thermosyphon drill bit, the variations could further assist in affirming the results achieved. It is also recommended that the manufacturing of thermosyphon drill bits be increased for an increased number of thermosyphon taper drills in order to ensure availability for conducting more trials to suit variations in drilling conditions. The availability of thermosyphon drills will ensure that more holes are drills consistently for the three tests that are required.

8.3 Conclusion

The objective of the study was the design and manufacturing of the thermosyphon drill that has the capacity to wick away heat from the drill bit tip, within drilling operations. The simulations that were conducted, where loads were applied on the drill bit to simulate a real life drilling condition, have assisted in giving light to the performance of the drill bits when drilling. These have led to a successful insertion of the thermosyphon within the drill bit. The simulation also

revealed the requirement for a larger web thickness that will facilitate the reverse tapered thermosyphon insertion.

The design carried out a careful calculation of the operating parameters which informed the simulation. The manufacturing process was thus successful and this assisted in the testing process being carried out. It is also noted that the exit temperatures that were measured from the drill bit cutting edges further solidified the success of the thermosyphon drill bit. Metal working fluids continue to affect employees within various machine shops, and this study has demonstrated the possibilities in heat transfer in drilling operations.

References

[1] T. C. Jen, F. Tuchowski, and Y. M. Chen, “Investigation of thermosyphon cooling for drilling operation: An experimental study,” *Am. Soc. Mech. Eng. Manuf. Eng. Div. MED*, vol. 16–1, pp. 59–67, 2008, doi: 10.1115/IMECE2005-82761.

[2] V. Muralidhar and P. K. Chaganti, “A review on testing methods of metalworking fluids for environmental health,” *Mater. Today Proc.*, no. xxxx, 2020, doi: 10.1016/j.matpr.2020.02.514.

[3] J. K. Mannekote, S. V. Kailas, K. Venkatesh, and N. Kathyayini, “Environmentally friendly functional fluids from renewable and sustainable sources-A review,” *Renew. Sustain. Energy Rev.*, vol. 81, no. June 2016, pp. 1787–1801, 2018, doi: 10.1016/j.rser.2017.05.274.

[4] J. Sequeira and T. C. Jen, “The Effect of Rotational Speed on Thermosiphon Cooling for the Application of Drill-bit Cooling,” *Procedia Manuf.*, vol. 7, pp. 211–217, 2017, doi: 10.1016/j.promfg.2016.12.052.

[5] T. L. Brzezinka *et al.*, “Hybrid Ti-MoS 2 coatings for dry machining of aluminium alloys,” *Coatings*, vol. 7, no. 9, pp. 1–13, 2017, doi: 10.3390/coatings7090149.

[6] S. Bhowmick and A. T. Alpas, “The role of diamond-like carbon coated drills on minimum quantity lubrication drilling of magnesium alloys,” *Surf. Coatings Technol.*, vol. 205, no. 23–24, pp. 5302–5311, 2011, doi: 10.1016/j.surfcoat.2011.05.037.

[7] O. Balzers, “With innovative PVD coating solutions for high-performance precision components,” pp. 0–7.

[8] W. V. A. N. Staden, “MANUFACTURE AND INVESTIGATION OF A TAPER THERMOSIPHON DRILL FOR DRY DRILLING,” no. October, 2017.

[9] L. Zhu, T. C. Jen, C. L. Yin, X. L. Kong, and Y. H. Yen, “Experimental analyses to investigate the feasibility and effectiveness in using heat pipe-embedded drills,” *Int. J. Adv. Manuf. Technol.*, vol. 58, no. 9–12, pp. 861–868, 2012, doi: 10.1007/s00170-011-3436-x.

[10] J. P. Byers, *Metalworking Fluids edited by*, 2nd Editio. 2016.

[11] F. Gorczyca, *Application of metal cutting theory*. New York: Industrial Press, 1987.

[12] D. P. Adler, W. W. Hii, D. J. Michalek, and J. W. Sutherland, “Examining the Role of Cutting Fluids in Machining and Efforts to Address Associated

Environmental / Health Concerns Shortened Title for Running Head," *Mach. Sci. Technol.*, vol. 10, no. 1, pp. 23–58, 2007.

[13] R. Rakić and Z. Rakić, "The influence of the metal working fluids on machine tool failures," *Wear*, vol. 252, no. 5–6, pp. 438–444, 2002, doi: 10.1016/S0043-1648(01)00890-0.

[14] J. P. Byers, *Metalworking Fluids*, Second. London, New York: Taylor and Francis Group, 2006.

[15] S. J. Skerlos, "PREVENTION OF METALWORKING FLUID POLLUTION : ENVIRONMENTALLY CONSCIOUS MANUFACTURING AT THE MACHINE TOOL PREVENTION THROUGH PROCESS," 2006.

[16] M. Schwarz, M. Dado, R. Hnilica, and D. Veverková, "Environmental and health aspects of metalworking fluid use," *Polish J. Environ. Stud.*, vol. 24, no. 1, pp. 37–45, 2015.

[17] N. A. Abdullah and Z. Hashim, "Metal Working Fluids (MWF) Aerosol in an Occupational Setting : Association with the Respiratory Symptoms and Lung Functions among Machinists .," vol. 4, no. 1, pp. 31–39, 2018.

[18] M. Mahdavi, S. Tiari, S. De Schampheleire, and S. Qiu, "Experimental study of the thermal characteristics of a heat pipe," *Experimental Thermal and Fluid Science*, vol. 93. pp. 292–304, 2018, doi: 10.1016/j.expthermflusci.2018.01.003.

[19] M. M. R. Nune and P. K. Chaganti, "Development, characterization, and evaluation of novel eco-friendly metal working fluid," *Meas. J. Int. Meas. Confed.*, vol. 137, pp. 401–416, 2019, doi: 10.1016/j.measurement.2019.01.066.

[20] M. S. Najiha, M. M. Rahman, and A. R. Yusoff, "Environmental impacts and hazards associated with metal working fluids and recent advances in the sustainable systems: A review," *Renew. Sustain. Energy Rev.*, vol. 60, pp. 1008–1031, 2016, doi: 10.1016/j.rser.2016.01.065.

[21] P. Kumar, S. A. H. Jafri, P. K. Bharti, and M. A. Siddiqui, "Study of Hazards Related To Cutting Fluids and Their Remedies," no. July, 2014.

[22] E. O. B. and D. L. Bennett, "Occupational airway diseases in the metalworking industry," pp. 169–176, 1985.

[23] T. Stefansson, "Application of Cryogenic Coolants in Machining Processes," pp. 1–51, 2014.

[24] E. Shakouri, H. Haghighi Hassanalideh, and S. Gholampour, "Experimental

investigation of temperature rise in bone drilling with cooling: A comparison between modes of without cooling, internal gas cooling, and external liquid cooling," *Proc. Inst. Mech. Eng. Part H J. Eng. Med.*, vol. 232, no. 1, pp. 45–53, 2018, doi: 10.1177/0954411917742944.

[25] A. Shokrani, V. Dhokia, and S. T. Newman, "Environmentally conscious machining of difficult-to-machine materials with regard to cutting fluids," *Int. J. Mach. Tools Manuf.*, vol. 57, pp. 83–101, 2012, doi: 10.1016/j.ijmachtools.2012.02.002.

[26] Y. Yildiz and M. Nalbant, "A review of cryogenic cooling in machining processes," *Int. J. Mach. Tools Manuf.*, vol. 48, no. 9, pp. 947–964, 2008, doi: 10.1016/j.ijmachtools.2008.01.008.

[27] N. Uçak and A. Çiçek, "The effects of cutting conditions on cutting temperature and hole quality in drilling of Inconel 718 using solid carbide drills," *J. Manuf. Process.*, vol. 31, pp. 662–673, 2018, doi: 10.1016/j.jmapro.2018.01.003.

[28] L. S. Ahmed and M. P. Kumar, "Cryogenic Drilling of Ti-6Al-4V Alloy Under Liquid Nitrogen Cooling," *Mater. Manuf. Process.*, vol. 31, no. 7, pp. 951–959, 2016, doi: 10.1080/10426914.2015.1048475.

[29] A. T. and A. D. A. Sharma, "Effects of Minimum Quantity Lubrication (MQL) in machining processes using conventional and nanofluis based cutting fluids: A comprehensive review," *J. Clean. Prod.*, vol. 127, pp. 1–18, 2016.

[30] M. Mosleh, K. Shirvani, S. Smith, J. Belk, and G. Lipczynski, "A Study of Minimum Quantity Lubrication (MQL) by Nanofluids in Orbital Drilling and Tribological Testing," *J. Manuf. Mater. Process.*, vol. 3, no. 1, p. 5, 2019, doi: 10.3390/jmmp3010005.

[31] B. Tasdelen, T. Wikblom, and S. Ekered, "Studies on minimum quantity lubrication (MQL) and air cooling at drilling," *J. Mater. Process. Technol.*, vol. 200, no. 1–3, pp. 339–346, 2008, doi: 10.1016/j.jmatprotec.2007.09.064.

[32] E. R. and H. Sasahara, "An analysis of surface integrity when drilling Inconel 718 using palm oil and synthetic ester under MQL condition," *Mach. Sci. Technol. Int. J.*, vol. 15, pp. 76–90, 2011.

[33] S. Bhowmick, M. J. Lukitsch, and A. T. Alpas, "Dry and minimum quantity lubrication drilling of cast magnesium alloy (AM60)," *Int. J. Mach. Tools Manuf.*, vol. 50, no. 5, pp. 444–457, 2010, doi: 10.1016/j.ijmachtools.2010.02.001.

[34] R. Kumar, H. Kumar Banga, H. Singh, and S. Kundal, "An outline on modern

day applications of solid lubricants," *Mater. Today Proc.*, vol. 28, pp. 1962–1967, 2020, doi: 10.1016/j.matpr.2020.05.558.

[35] R. Li and A. J. Shih, "Tool temperature in titanium drilling," *J. Manuf. Sci. Eng. Trans. ASME*, vol. 129, no. 4, pp. 740–749, 2007, doi: 10.1115/1.2738120.

[36] A. Faghri, "Heat Pipes: Review, Opportunities and Challenges," *Front. Heat Pipes*, vol. 5, no. 1, 2014, doi: 10.5098/fhp.5.1.

[37] R. S. Gaugler, "Heat Transfer Device. U. S. Patent 2,350,348.," 1944.

[38] B. Zohuri, *Heat Pipe Design and Technology*, Second. Albuquerque, NM, USA: Springer International Publishing, 2016.

[39] T. Cotter, "Theory of heat pipes," *Los Alamos Sci. Lab. Rep.*, no. No. LA-3246, 1965.

[40] C. W. Chan, E. Siqueiros, J. Ling-Chin, M. Royapoor, and A. P. Roskilly, "Heat utilisation technologies: A critical review of heat pipes," *Renew. Sustain. Energy Rev.*, vol. 50, pp. 615–627, 2015, doi: 10.1016/j.rser.2015.05.028.

[41] J. Strain, "EXPERIMENTAL COMPARISON OF HEAT PIPES AND THERMOSYPHONS CONTAINING METHANOL AND by EXPERIMENTAL COMPARISON OF CONTAINING METHANOL AND," *A Thesis*, p. 214, 2017.

[42] A. Faghri, *Heat Pipe Science and Technology*, Second. United States of America: Global Digital Press, 2016.

[43] H. Shabgard, M. J. Allen, N. Sharifi, S. P. Benn, A. Faghri, and T. L. Bergman, "Heat pipe heat exchangers and heat sinks: Opportunities, challenges, applications, analysis, and state of the art," *Int. J. Heat Mass Transf.*, vol. 89, pp. 138–158, 2015, doi: 10.1016/j.ijheatmasstransfer.2015.05.020.

[44] C. C. Silverstein, *Design and Technology of Heat Pipes for Cooling and Heat Exchange*. Washington, 1992.

[45] F. Gunnerson, K. Weaver, and K. Weaver, "Theoretical Design of a Thermosyphon for Efficient Process Heat Removal from Next Generation Nuclear Plant (NGNP) for Production of Hydrogen," *Idaho Natl. Lab.*, no. October, 2007.

[46] T. C. Jen, F. Tuchowski, and Y. M. Chen, "Investigation of Thermosyphon Cooling for Drilling Operation : An Experimental Stndy," *Am. Soc. Mech. Eng. Manuf. Eng. Div. MED*, vol. 16–1, pp. 59–67, 2008, doi: 10.1115/IMECE2005-82761.

[47] P. K. David Reay, *Heat Pipes theory, design and applications*, Fifth. Linacre

House, Jordan Hill, Oxford OX2 8DP: Butterworth Heinemann, 2006.

[48] B. Fadhl, “Modelling of the Thermal Behaviour of a Two-Phase Closed Thermosyphon,” no. March, p. 184, 2015.

[49] L. J. Ballback, “The Operation of a Rotating, Wickless Heat Pipe,” no. March, p. 53, 1969.

[50] E. M. Sparrow and J. P. Hartnett, “Condensation on a rotating cone,” *J. Heat Transfer*, vol. 83, no. 1, pp. 101–102, 1961, doi: 10.1115/1.3680454.

[51] H. Nguyen-Chi and M. Groll, “Entrainment or flooding limit in a closed two-phase thermosyphon,” *J. Heat Recover. Syst.*, vol. 1, no. 4, pp. 275–286, 1981, doi: 10.1016/0198-7593(81)90038-2.

[52] A. C. Gurses, C. Cannistraro, and L. Tezcan, “The inclination effect on the performance of water-filled heat pipes,” *Renew. Energy*, vol. 1, no. 5–6, pp. 667–674, 1991, doi: 10.1016/0960-1481(91)90012-E.

[53] R. Shanthi and V. Ramalingam, “Performance of Two Phase Gravity Assisted Thermosyphon Using Nanofluids,” *Front. Heat Pipes*, vol. 5, no. 1, 2014, doi: 10.5098/fhp.5.3.

[54] T. C. Jen, Y. M. Chen, and G. Gutierrez, “Thermal Performance of Heat Pipe Drill: Experimental Study,” *Proc. ASME Summer Heat Transf. Conf.*, vol. 2003, no. 1987, pp. 87–93, 2003, doi: 10.1115/ht2003-47096.

[55] T. C. Jen *et al.*, “Investigation of heat pipe cooling in drilling applications. Part I: Preliminary numerical analysis and verification,” *Int. J. Mach. Tools Manuf.*, vol. 42, no. 5, pp. 643–652, 2002, doi: 10.1016/S0890-6955(01)00155-9.

[56] Sandvik Coromant, “Machining formulas and definitions,” 2019. https://www.sandvik.coromant.com/en-gb/knowledge/machining-formulas-definitions/pages/drilling.aspx (accessed Dec. 10, 2019).

[57] M. P. Groover, *Principles of Modern Manufacturing*. Singapore: John Wiley & Sons, 2013.

[58] Sandvik Coromant, “Machining formulas and definitions,” *Machining formulas and definitions*, 2019. https://www.sandvik.coromant.com/en-gb/knowledge/machining-formulas-definitions/pages/drilling.aspx (accessed Mar. 01, 2019).

[59] M. . Fagan, *Finite Element Analysis. Theory and Practice*. England: Longman Group UK Limited, 1992.

[60] T. Tharayil, L. Godson, V. Ravindran, and S. Wongwises, “Effect of filling ratio

on the performance of a novel miniature loop heat pipe having different diameter transport lines," *Appl. Therm. Eng.*, vol. 106, pp. 588–600, 2016, doi: 10.1016/j.applthermaleng.2016.05.125.

[61] L. Zhu, T. C. Jen, Y. B. Liu, J. W. Zhao, W. L. Liu, and Y. H. Yen, "Cutting tool life analysis in heat-pipe assisted drilling operations," *J. Manuf. Sci. Eng. Trans. ASME*, vol. 137, no. 1, pp. 1–8, 2015, doi: 10.1115/1.4028481.

[62] L. Zhu, T. C. Jen, C. L. Yin, X. L. Kong, and Y. H. Yen, "Experimental analyses to investigate the feasibility and effectiveness in using heat-pipe embedded end-mills," *Int. J. Adv. Manuf. Technol.*, vol. 60, no. 5–8, pp. 497–504, 2012, doi: 10.1007/s00170-011-3629-3.

[63] T. Jen and Y. Chen, "HT2003-40096 Thermal Performance of Heat Pipe Drill : Experimental Study," no. 1987, pp. 1–7, 2003.

[64] S. W. C. C. Tools, "E1 Somta Catalogue," 2019. http://www.somta.co.za/pdf/somta-user-guide.pdf (accessed Oct. 01, 2019).

[65] B. E. Centre, "BRITISH STAINLESS STEEL ASSOCIATION," 2019. https://www.bssa.org.uk/topics.php?article=194 (accessed Oct. 20, 2019).

[66] A. Technologies, "AU Series," 2019. https://www.bhktrading.com/uploads/1/8/4/6/18465418/au_series.pdf (accessed Oct. 25, 2019).

[67] M. Simon, L. Grama, P. Maior, T. Mureș, N. Iorga, and T. Mureș, "STUDIES FOR OBTAINING A SMALL HOLLE , RAPID EDM DRILLING MACHINE," pp. 197–199, 2011.

[68] T. I. Company, *Zeus Precision*. PO Box 59, Jersey British Channel Islands: Seel House Press Liverpool, 1976.

[69] E. Toolbox, "Thermal Conductivity of Metals, Metallic Elements and Alloys," 2005. https://www.engineeringtoolbox.com/thermal-conductivity-metals-d_858.html (accessed Nov. 01, 2019).

[70] L. Zhu, T.-C. Jen, C.-L. Yin, X.-L. Kong, and Y.-H. Yen, "Investigation of the feasibility and effectiveness in using heat pipe-embedded drills by finite element analysis," *Int. J. Adv. Manuf. Technol.*, 2013, doi: 10.1007/s00170-012-4077-4.

[71] P. Brown, M. Evans, D. Hunt, J. McIntosh, B. Pender, and J. Ramagge, "Cones, Pyramids and Spheres," *Aust. Math. Sci. Inst.*, no. June, 2011.

[72] K. Sunt and J. H. Lienhardj, "THE PEAK POOL BOILING HORIZONTAL ON," vol. 13, 1970.

[73] F. P. Incropera;, D. P. Dewitt;, T. L. Bergman;, and A. S. Lavine, *Fundamentals of Heat and Mass Transfer*, Sixth., vol. 112. 111 River Street, Hoboken, NJ 07030-5774: John Wiley & Sons, 2007.

[74] Lucider, “Convert revolutions per minute to radians per second,” 2020. https://lucidar.me/en/unit-converter/rad-per-second-to-revolution-per-minute/ (accessed Oct. 10, 2020).

[75] and H. H. R. Erik Oberg, Franklin D. Jones, Holbrook L. Horton, *Machinery ’ s Handbook*, 28th ed. New York: Industrial Press Inc.

[76] G. Hao and Z. Liu, “The heat partition into cutting tool at tool-chip contact interface during cutting process: a review,” *Int. J. Adv. Manuf. Technol.*, vol. 108, no. 1–2, pp. 393–411, 2020, doi: 10.1007/s00170-020-05404-9.

[77] M. C. Shaw and J. O. Cookson, *Metal cutting principles (Vol. 2)*, Second., no. June. 198 Madison Avenue, New York, 10016: Oxford University Press, Inc., 2005.

[78] S. W. C. C. Tools, “E1 Somta Catalogue,” 2019. .

Appendices

Appendix A

Calculation of the drilling conditions

The testing method was conducted on a selected speed of 245 rev/min for the tests conducted.

$$N = \frac{v}{\pi D} \tag{1}$$

Substituting the variables, the cutting speed is therefore:

$$v = \frac{\pi N D}{1000}$$

$$= \frac{\pi(245)(20)}{1000}$$

$$= 15.3938 \text{ m/min}$$

The feed is calculated with the following equation:

$$f = N f_r \tag{2}$$

Substituting the variables, the feed is therefore:

$$f = (245)(0.0254)$$

$$= 6.223 \text{ mm/min}$$

The drilling time is calculated using the following equation:

$$T_m = \frac{t + A}{f_r} \tag{3}$$

*A*is the approach allowance in (mm), and this is calculated using the following equation;

$$A = 0.5D \tan\left(90 - \frac{\theta}{2}\right) \tag{4}$$

Where, the point angle of the armour piercing drill is 130º.

Substituting the variables, the approach allowance is therefore:

$$A = 0.5 \times 20 \times \tan\left(90 - \frac{130}{2}\right)$$

$$= 4.663 \text{ mm}$$

The thickness of the work piece for the test is 30 mm.

Substituting the variables, the machining time is therefore:

$$T_m = \frac{t + A}{f}$$

$$= \frac{50 + 4.663}{6.223}$$

$$= 5.57 \text{ min}$$

The material removal rate is calculated using the following equation:

$$R_{MR} = \frac{\pi D^2 f_r}{4} \quad (5)$$

Substitution the variables, the material removal rate is:

$$= \frac{\pi(20)^2(0.0254)}{4}$$

$$= 7.9796 \text{ cm}^3/\text{min}$$

The specific cutting force is calculated using the following equation:

$$K_C = K_{C1}(f_z \times \sin(k_r))^{-mc}\left(1 - \frac{\gamma}{100}\right) \quad (6)$$

Where:

$K_C$is the specific cutting force in(N/mm^2)

$K_{C1}$is 1500

$f_z$is the feed force in the z direction and it is worked out as follows:

$$f_z = \frac{f_r}{2} \quad (7)$$

$$= \frac{0.0254}{2}$$

$$= 0.0127$$

Where:

$k_r$is the pointing angle (which is 130°) and when divided by 2 the angle is 65°.

$mc$is 0.25

$\gamma$is the rake angle or helix angle which is 15°.

Substituting the variables, the specific cutting force is therefore:

$$= 1500(0.0127 \times \sin(65))^{-0.25}\,(1 - \frac{15}{100})$$

$$= 3892.6 \text{ N/mm}^2$$

The feed force or thrust force is calculated using the following equation:

$$F_T = 0.5 \times K_C \times \frac{D}{2} \times f_r \times \sin(k_r) \quad (8)$$

Substituting the variables, the feed force is therefore:

$$F_T = 0.5 \times 3892.6 \times \frac{20}{2} \times 0.0254 \times \sin(65)$$

$$= 448.04 \text{ N}$$

The net power required, is calculated using the following equation:

$$P_C = \frac{f_r \times v \times D \times K_C}{240 \times 10^3} \quad (9)$$

Substituting the variables, the net power is therefore:

$$P_C = \frac{0.0254 \times 15.394 \times 20 \times 3892.6}{240 \times 10^3}$$

$$= 0.127 \text{ kW}$$

The torque is calculated using the following equation:

$$M_C = \frac{P_C 30 \times 10^3}{\pi N} \quad (10)$$

Substituting the variables, the torque is:

$$M_C = \frac{(0.127)(30 \times 10^3)}{\pi \times 245}$$

$$= 4.9 \text{ Nm}$$